The Strutjet Rocket Based Combined Cycle Engine

A. Siebenhaar and M.J. Bulman
GenCorp Aerojet
Sacramento, CA

And

D.K. Bonnar
Boeing Company
Huntington Beach, Ca

TABLE OF CONTENTS

List of Tables

List of Figures

1.0 Introduction

The multi-stage chemical rocket has become established over many years as the propulsion system for space transportation vehicles, while, at the same time, there is increasing concern about its continued affordability and rather involved reusability. Two broad approaches to addressing this overall launch cost problem consist in one, the further development of the rocket motor, and two, the use of airbreathing propulsion to the maximum extent possible as a complement to the limited use of a conventional rocket. In both cases, a single-stage-to-orbit (SSTO) vehicle is considered a desirable goal. However, neither the "all-rocket" nor the "all-airbreathing" approach seems realizable and workable in practice without appreciable advances in materials and manufacturing. An affordable system must be reusable with minimal refurbishing on-ground, and large mean time between overhauls, and thus with high margins in design. It has been suggested that one may use different engine cycles, some rocket and others airbreathing, in a combination over a flight trajectory, but this approach does not lead to a converged solution with thrust-to-mass, specific impulse, and other performance and operational characteristics that can be obtained in the different engines. The reason is this type of engine is simply a combination of different engines with no commonality of gas flowpath or components, and therefore tends to have the deficiencies of each of the combined engines. A further development in this approach is a truly combined cycle that incorporates a series of cycles for different modes of propulsion along a flight path with multiple use of a set of components and an essentially single gas flowpath through the engine. This integrated approach is based on realizing the benefits of both a rocket engine and an airbreathing engine in various combinations by a systematic functional integration of components in an engine class usually referred to as a rocket-based combined cycle (RBCC) engine.

RBCC engines exhibit a high potential for lowering the operating cost of launching payloads into orbit. Two sources of cost reductions can be identified. First, RBCC powered vehicles require only 20% takeoff thrust compared to conventional rockets, thereby lowering the thrust requirements and the replacement cost of the engines. Second, due to the higher structural and thermal margins achievable with RBCC engines coupled with a higher degree of subsystem

redundancy lower maintenance and operating cost are obtainable. Both these reductions result from the increased specific impulse of RBCC engines and the reduction in takeoff and dry mass.

The Strutjet engine is described in detail in Section 2, along with the delineation of five modes of engine operation, optimization of the propulsion system, and the resulting engine architecture. Section 3 is devoted to integration of the engine with the flight vehicle, and also addresses the performance of the engine as a propulsion system and in relation to various types of flight vehicles. In addition the concept of robustness space is utilized to assess the design of the engine and its ability to reduce operations cost. Section 4 deals with the testing accomplished to-date and future plans for on-ground and flight vehicle testing. Section 5 addresses the maturity of various elements of the overall RBCC technology. Finally, the applicability and superior potential of the Strutjet engine, as a leading rocket-based combined cycle engine for potentially low operating cost launch vehicles, is summarized in Section 6.

2. Strutjet Engine

The Aerojet Strutjet engine is a member of the RBCC class of engines with several new technologies and innovations. Many of these technologies are also of far reaching interest in other propulsion schemes. The Strutjet engine operates all of the cycles with liquid hydrogen (LH2) for fuel, and liquid oxygen (LOX) and atmospheric air as necessary for combustion of fuel.

The name *Strutjet* is derived from the use of a series of struts in the front part of the engine flowpath. The struts serve a number of functions in the engine, including compression of incoming air, isolation of combustion from air inlet (that is, as an isolator), fuel distribution and injection, ram/scram combustion, and rocket-thruster integration in the different modes of engine operation. The struts finally provide efficient structural support for the engine. The struts thus form a key element in the engine.

The Strutjet engine is in principle, a single engine configuration with three propulsion elements, namely rocket, ramjet, and scramjet in its five mode operation. The elements are highly integrated in design and function. Engines of related conceptual designs have been considered for similar applications by W.J.D. Escher and B.J. Flornes[1] and also by F. Billig and D. Van Wie[2] in a US patent for an RBCC type engine. The Billig-Van Wie engine has a separate inlet for compression and then uses struts downstream for the purpose of distributing various fuel injectors across the flow path. The difference between such earlier concepts and the Aerojet Strutjet is found in the higher degree of functional integration of various Strutjet engine components which results in a shorter, higher thrust-to-weight engine with good performance. The specific impulse of the Strutjet engine is characteristic of other known airbreathing engines without the thrust-to-mass penalty of having separate propulsion systems for different flight conditions.

The Strutjet engine concept is founded on obtaining specific impulse, I_{sp}, higher than that of a rocket, a better thrust-to-mass ratio ($F m_e$) than an all-airbreathing engine, and a substantial reduction in vehicle gross take-off-weight, GTOW. Thus the mean I_{sp} for the

Strutjet is estimated to be 586 sec. while the conventional hydrogen-oxygen rocket provides I_{sp} of 425 sec. In comparison, the mean I_{sp} for an all-airbreather such as the USA National AeroSpace Plane (NASP) was estimated to be 755 sec. A SSTO-type all-rocket may yield F/m_e equal to 80 lbf/lbm and a NASP-type SSTO all-airbreather, about 6 lbf/lbm. Using current state-of-the-art technology, a strutjet can be built with F/m_e of 35 lbf/lbm; however, as shown later, for the sake of increased engine robustness, F/m_e values as low as 25 lbf/lbm are employed in the analysis. The GTOW, made up of the empty weight, propellant, and payload, becomes reduced for a Strutjet due to the reduction in the amount of oxygen that needs to be carried on board at vehicle launch. It is expected that the propellant mass fraction can be maintained at the present state-of-the-art levels, about 85%, compared to the required 90% value, for an all-rocket SSTO system. At the same time the engine and the launch vehicle are expected to have substantially higher structural reliability margins than the all-rocket and the all-airbreathing engine system. Finally, the thermal management of these vehicles can also be accomplished within the current state-of-the-art because high-speed atmospheric airbreathing operation is limited to a relatively low Mach number such as 10. This avoids the severe vehicle heating conditions that are known to have imposed serious engineering challenges, typical for hypersonic atmospheric flight in the regime above Mach 10 in NASP-type vehicles. The Strutjet vehicle trajectory is chosen such that the ascent thermal loads are equal to or less than the thermal loads that a reusable vehicle would experience during reentry.

2.1 Flow Path Description

Figure 1 provides a schematic of the Strutjet and identifies the different elements in the combined cycle engine. The propulsion subsystems are integrated into a single engine using common propellant feed lines, cooling systems, and controls. The air inlet along with the struts, the combustion sections, and the nozzle make up the main engine flow path. An isometric view of a typical RBCC Strutjet engine is given in Figure 2.

2.2 Engine Architecture

2.2.1 Flow Path Elements

The variable geometry inlet incorporates two engine ramps, that maximize air capture and control compression as required by the engine. The inlet combines effective forebody precompression with strut compression. This results in "soft start", low spill drag, and good capture and recovery efficiencies. The "soft start" is a result of the increased openness of the inlet on the cowl side, which causes a gradual decrease in spillage with increasing Mach number. This, in turn, provides smooth increases in captured air mass flow and pressure recovery.

The inlet geometry and the changes in contraction ratio as a function of flight Mach number are shown in Figure 3. The struts or flow dividers, which extend into the inlet, channel the flow into discrete, narrow flowpaths that diffuse the flow over the shortest length possible. In the forward part of the inlet, where the struts are designated as "windscreens", the air capture is enhanced by locating the cowl lip near the minimum flow area section (variable geometry wide open); this also facilitates inlet start at low supersonic speeds. The struts are integrated in the inlet such that each flow passage between two adjoining struts behaves like a sidewall compression inlet, and provides what may be called "strut compression". Past the cowl lip, at low speeds, the flow area between two adjacent struts remains constant; the strut section serves as an inlet combustor isolator during ducted rocket and ramjet mode. At higher speeds ($M \approx 5$) the inlet ramps are deployed to increase the engine contraction and performance.

Above Mach 6 the scram mode is the most efficient and the diverging isolator duct between the fully contracted inlet throat and the rockets is used as the scram combustor. During this mode of operation the variable nozzle geometry adjusts the scram combustor flowpath into a continuously diverging configuration.

Maximum engine performance is achieved when the fuel is injected as far forward as possible without degrading the inlet air capture capability. In general, this requires the fuel

injection point to start well back in the flowpath and move continuously forward as the vehicle accelerates. Ideally, this would imply an infinite number of injectors which would be turned on or off as the Mach number changes. The Strutjet flowpath employs three stages of fuel injection to cover this range. These injectors are referred to as the base axial, aft and forward injectors. The base axial injectors delay the heat release at low speeds until the flowpath area is large enough to tolerate it. The rockets used in the boost phase of the mission and the ascent phase are housed in the trailing end of the main struts. These strut rockets also integrate two of the airbreathing injector stages. At intermediate speeds, the aft (ram) injectors are employed in combination with one of the other injectors to control the effective heat release location as required in order to maximize the engine performance. At high scram speeds, the fuel is injected from the forward (scram) injectors in order to complete the combustion before the fuel can leave the engine.

The ram combustor used at speeds up to Mach 6, is located aft of the strut rockets. This combustor provides enough area to permit stoichiometric subsonic combustion at low speeds.

The Strutjet variable geometry nozzle is a simple flap used to control subsonic combustion pressure to create the optimum thrust as dictated by operating mode and flight Mach number. This nozzle flap is the principle control in the transition to the scram mode. By opening the nozzle flap up at approximately Mach 6, the combustor pressure drops and the flow remains supersonic through the combustor.

2.2.2 Turbomachinery, Propellant Supply & Thermal Management

Turbomachinery, in particular the liquid hydrogen fuel pump, may be considered the Achilles heel of high-performance rocket engines. Unlike the conventional rocket engine, the Strutjet provides high performance without relying on the cutting-edge turbomachinery technology, particularly the use of advanced, high-strength, high-temperature materials. The demands on the Strutjet fuel turbopump are significantly lower relative to the conventional rocket as summarized in Table 1. This contributes significantly to increased reliability, extended life, and reduced cost of the Strutjet engine operation.

During the ducted rocket mode. the engine fuel supply is powered by a fuel-rich gas generator exhausting into the ram-scram duct through the base axial injectors. while the oxygen supply is powered by an oxidizer-rich staged combustion cycle. In contrast to the hydrogen side. stage combustion on the oxygen side does not impose a technical challenge since oxygen. being a high density fluid. can be pumped to the required pressure levels at relatively benign shaft speed. Oxygen-rich preburner technology provides advantages of reduced turbine temperature and elimination of interpropellant seals needed for fuel-rich gas-driven oxygen pumps. Figure 4 illustrates the engine cycle during the ducted rocket mode of operation. During pure airbreathing modes. the entire oxygen feed system is. of course, inactive. As shown in Figure 5, the fuel side operates now in a simple expander cycle mode using heat available from the required cooling of the engine structure. In the scram-rocket mode the fuel remains operating in the expander cycle and the oxidizer circuit is restarted in the staged combustion cycle, as shown in Figure 6. Figure 7 illustrates the location of these various operating modes on the fuel pump operation map.

2.2.3 Engine Cycle

The overall Strutjet engine propellant flow is illustrated in the previously shown Figure 4. As displayed. there are three subsystems: (i) the hydrogen and oxygen fuel tanks, turbopumps feed system and powerhead; (ii) the strutrocket and fuel injection assembly, and (iii) the engine structure and cooling system. Both the strut rocket and the engine structure are operating in the thermal and combustion gas dynamic environment.

Fuel rich gases generated in the fuel gas generator (FGG) drive the hydrogen turbine, and are subsequently injected into the engine internal air stream at selected locations through base-axial, aft, and forward injectors. The selection depends on the engine operating mode. and is accomplished through appropriate valving. Hydrogen gas is also used to cool the rocket chambers (the figure including representationally only one) and the engine structure before injection into the combustor section. In the expander cycle. hydrogen heated by the engine structure bypasses the preburner and drives the turbine in an expander cycle.

The oxygen side of the propellant system is only active during rocket operation. and operates (always) in a stage-combustion cycle. The oxygen rich turbine drive gases are

7

generated in the preburner (OPB) through the burning of a small amount of hydrogen and all of the oxygen flow. prior to injection into the rocket chambers.

The table shown in Figure 4 includes four attributes for each of the five operating modes:

(i) selected power cycle in the oxygen and hydrogen supplied.

(ii) amount of rocket propellant flow.

(iii) amount of hydrogen injected into the air stream. and

(iv) settings of the inlet and nozzle variable geometry.

2.2.4 Structural Concept

The struts provide a very efficient means for a number of processes: First the struts are an important structural element of the engine. They reduce the unsupported spans and reduce weight. and enhabce fuel injection. mixing, and combustion at supersonic speeds. They also incorporate the strut rockets. These compact rockets serve to induce air flow and to assist in air-fuel mixing in the ducted rocket mode. When operative, they provide the bulk of the thrust.

The current design employs additional Aft Struts in the aft-end of the combustion zone, which gives rise to a substantial engine panel mass reduction. These engine panels are essentially two-layer "laminates" comprised of a structural and a thermal protection layer. Minimization of the total panel weight over the entire engine is accomplished by optimizing the design of each of these layers. In the case of the structural layer, substantial mass savings can also be realized by incorporating. where possible. supporting structures to reduce the unsupported panel span. In the inlet-isolator the main engine struts inherently serve as supporting structures. However. the strut rockets define the end of the main struts. leaving a large. unsupported panel. Structure weight-trade studies have shown that the panel mass in the combustion region can be reduced by adding several Aft Struts into this region. as shown in Figure 8. Note that the amount of weight savings. relative to the number of additional struts diminishes as the number of Aft Struts increases. due to their own weight. As shown in Figure 1. the present Strutjet engine design incorporates 6 Aft Struts. with a ram combustor panel mass saving of nearly 80% compared to a configuration with no aft struts. Based on symmetric design

8

considerations, a set of 11 Aft Struts would be the next possible configuration; but this would substantially increase internal engine drag and heat load on the cooling system, without a corresponding payoff in structural weight savings. The achievable engine thrust-to-mass using advanced technology is as high as 35lbf/lbm.

2.3 Strutjet Operating Modes

Along a typical SSTO ascent trajectory a Strutjet operates in five modes with smooth transition between modes:

I. ducted rocket operation for takeoff and acceleration through the transonic speed regime into the supersonic region;

II. ramjet operation from Mach 2.5 to about 6;

III. scramjet operation from Mach 6 into the hypersonic speed range up to Mach 10;

IV. scram /rocket operation from Mach 10 to low vacuum conditions; and

V. ascent rocket from low vacuum operation up to orbital speeds.

2.3.1 Ducted Rocket Mode

Before discussing the ejector ramjet concept employed in the Strutjet, it will be helpful to revisit two known, classical ejector ramjet concepts[3]. The most efficient of the two is the socalled "Diffuse and Afterburn" (DAB) concept which employs a sequential series of the ejector processes. This is more thermodynamically efficient but has substantial adverse consequences. To prevent premature combustion during the ejector pumping (driven by shear mixing between primary and secondary flows) and diffusion, stoichiometric or oxygen rich rocket mixture ratios are needed. This reduces the rocket Isp and is a challenge for the cooling system. Since no available fuel is entrained in the rocket exhaust, separate fuel injectors are required in the large area of the ram burner. This approach adds significant length and weight to the engine.

The second type of ejector ramjet is called the "Simultaneous Mix and Combust" (SMC). In this type Ejector Ramjet, the processes are allowed to occur in parallel in a shorter duct. The fuel for afterburning comes from the conventionally fuel rich rocket exhaust. After burning

begins immediately and a diverging duct is needed to keep from drastically reducing the air induction due the thermal occlusion. Although shorter and lighter. this approach loses up to 30% of the thrust of the DAB Ejector Ramjet at take off.

The Strutjet combines the best of each of these historic ejector ramjets. Here. the duct is as short as the SMC but with the performance close to the DAB type. To realize a short duct length. the flowpath is divided up into many narrow gaps by the struts. The ejector pumping occurs between the struts and is complete much faster than without struts. The diffusion occurs in the other plane by the divergence of the body wall. The rockets are operated at a high but still fuel rich mixture ratio. The body wall divergence provides the needed tolerance to the incidental combustion of this fuel. The bulk of the fuel (provided in the fuel rich turbine exhaust) for afterburning is injected from the base of the struts. In order to maintain high performance, the amount of air the strut rockets can induct into the ram combustor must be maximized. The artifice employed is to reduce the rate of early heat release. Figure 9 shows the performance loss due to reduced air ejection as a function of the amount of air burned at the front of the ram combustion zone. To prevent the performance loss from early heat release in the ram combustion two strategies are employed. One, the amount of free hydrogen in the rocket exhaust is minimized, minimizing the amount of fuel which can come in contact with air in the front part of the ram combustion zone, the strut rockets are designed to operate near stoichiometric conditions with only a small amount of fuel film cooling. The second strategy consists in delaying the afterburning of the turbine exhaust. The fuel rich turbine exhaust is injected into the ram combustion chamber from the base of the struts between the rocket nozzles as illustrated in Figure 10. This fuel rich turbine exhaust is buried inside the rocket plumes. After the diffusion is complete. when the heat release can be tolerated. the turbine exhaust emerges from the rocket plumes and burns with the air in the ramburner. Complex auxiliary injectors and flame holders are thus avoided. This concept is illustrated in Figure 11. In this mode, the engine inlet is wide open. and the nozzle is in a partially closed position that is chosen, to maximize the engine thrust.

The ducted rocket mode provides some added specific impulse over an all-rocket engine up to Mach 2.5. where the ramjet mode takes over.

Mode I.a: During the ducted rocket mode, the variable geometry inlet is wide open. Figure 10 provides an upstream view into the combustion zone. As can be seen, three base axial injectors are located at the strut base between four rocket thrusters. Under take-off conditions when maximum thrust is required, the strut rockets are operated at maximum chamber pressure. Since operation in the ducted rocket mode consumes a significant proportion of the propellant on-board the vehicle, increasing performance with induced air (thrust augmentaion) is considered essential, and contributes to the high mission-average specific impulse required by Earth-to-orbit vehicles.

Mode I.b: At higher flight speeds in ducted rocket mode, additional fuel is injected into the combustion zone through the Aft Injectors. Figure 10 shows the location of these injectors and also illustrates how the fuel distribution can be tailored in a direction normal to air flow in the combustion zone, so as to match the fuel flow to the locally available air flow.

2.3.2 Ramjet Mode

Struts provide an ideal mounting place for ram and scram injectors. Combustion efficiencies up to 95 percent have been demonstrated with both hydrocarbon and hydrogen fuels at Mach 8 conditions at high fuel equivalency ratios, at which it is most difficult to burn completely. Figure 12 illustrates how strut-mounted injectors reduce the "mixing gap", thus allowing a significant reduction in combustor length and weight. The Strutjet's shorter combustion zone has lower internal drag and reduced heat load. In the case of hydrogen, a cascade fuel injector has been specifically designed for the injection of gaseous hydrogen in the Scramjet. A cascade injector[4] delivers the fuel in the form of a low drag wedge shaped fuel plume. The fuel is injected normally at supersonic speed into the supersonic airstream, the injectors being tailored such that the injected gas is expanded to a level close to the ambient static pressure in the combustor, thereby realizing a low drag shape and increased momentum. In addition to its superior penetration and mixing, shown in Figure 13, a cascade injector reduces the wall heat flux near the injector by a factor of five or more by avoiding the classic separation bubble found in front of a high drag normal fuel jet. The reduction of these injection-induced hot spots reduces the cooling system complexity and pressure drop.

The predicted airbreathing I_{sp} performance shown in Fig. 7 can only be obtained in a practical engine if high combustion efficiency is achieved. Whereas the efficient generation of thrust, even in large area rocket engines, is well understood, the maximization of ram-scram combustion efficiency and thrust generation, being primarily a function of the fuel injection scheme, is a technical challenge: however, a practical strategy is now well in hand. The Strutjet fuel injection schemes provide the required flexibility of timing and location of the heat release without significant total pressure loss.

Modes I.c and II: Prior to, and during transition, and in the ramjet mode, engine cooling provides enough energy to the hydrogen in the cooling circuit, and the gas generator can be turned off: the rocket then operates on the fuel side in an expander cycle. When full ramjet operation is achieved, the rocket fuel and oxidizer circuits are shut down and the fuel to the "ram and scram" injectors is controlled such that combustion moves forward as Mach number increases. Ramjet take over occurs at Mach 2.5. This low Mach number is due to the high capture efficiency and low design point of the Strutjet engine. At flight speeds beyond Mach 3, the inlet ramps are deployed to gradually increase contraction, eventually reaching full contraction before scram transition.

In low ramjet mode, the Strutjet variable geometry remains open to maximize air capture and thrust; however, the nozzle opening is dictated by the desired ramjet burner pressure. The strut rockets are turned off. As described earlier, no turbine exhaust gas is available in this mode. The desired combustion location (location of highest pressure) is downstream from the struts in the ram combustion area. For this case, two injection sites, one normal injector at the aft end of the isolator section, see top of Figure 1, and a second axial injector in the strut rocket base, see Figure 10, are provided. The available injection sites permit heat release optimization through a division of fuel flow rates between the two principal injection sites, referred to as the aft and base axial injectors.

2.3.3 Scramjet Mode

Mode III: During transition from ramjet to scram mode the nozzle is opened fully, and some of the fuel is injected from the forward injectors. In scram mode, the geometry in the engine internal flow path is similar to that in the ram mode except now the inlet is fully contracted and the combustion nozzle is wide open. The flow through the engine is supersonic, the highest pressure location being in the flow isolator section between the struts. The combustion control options are similar to those of the ram mode with the injection shifted forward. Heat release is controlled by regulating the fuel flow between the forward and aft injectors. At the high scram Mach numbers of 7 to 10, the aft injectors are turned off and all the fuel is injected through the forward injectors. These are located downstream of the inlet throat as seen in Figure 1 and are vertically arranged as indicated in Figure 10.

2.3.4 Scram/Rocket and Ascent Rocket Modes

The end of Strutjet air-breathing operation begins with a pitch up maneuver taking the vehicle outside the sensible atmosphere. This maneuver is initiated with the strut rockets re-ignited while the scram engine is still producing significant thrust. The rocket operation gives rise to scramjet performance benefits from the additional contraction of the incoming air caused by the displacement of the rocket plume gases. At Mach 10 such combined operation results in roughly twice the engine thrust as either element operating alone. This synergy is very beneficial at this point in flight time, as large thrust is needed to overcome the increased drag associated with the pitch up maneuver.

Modes IV and V: During transition from scram to scram-rocket and then to ascent rocket mode, the rocket operates in the same cycle as during the transition to the ram mode. When the flight dynamic pressure falls below internal engine pressure the inlet is closed off completely to prevent the rocket gases from escaping out the front. The scram injectors operate at a small flow rate to provide some bleed flow which cools the Strutjet inlet and isolator sections forward of the rockets, and which also minimizes attachment shocks of the rocket exhaust plumes. During this

13

operation, the nozzle is kept wide open, as stated earlier, in order to provide the maximum rocket gas expansion possible. With the inlet closed off, this results in a very large nozzle area ratio nozzle that expands its exhaust products over the boattail of the vehicle. This generates the highest possible rocket specific impulse. A very important parameter in the design of an RBCC vehicle is the selected transition Mach number (M_t). It impacts the mission average specific impulse, engine/vehicle weights and correspondingly the vehicle GTOW. For the sake of system robustness and associated increased system reusability a lower transition Mach number, $M_t \leq 10$, is advantageous because it exposes the vehicle and engine to lower heat loads. For the vehicle discussed in this chapter a transition Mach number of 10 has been baselined. Beyond this the rocket is re-ignited and during this submode, referred to as scram/rocket mode, the vehicle begins its pull-up out of the atmosphere; the scram/rocket operation provides an addition of 5 seconds to the mission average I_{sp}. At approximately Mach 12 (and a dynamic pressure about 25 psf) the inlet is closed off and the engine operates beyond that point in the ascent/rocket mode as a high area ratio rocket.

2.4 Optimal Propulsion System Selection

An optimal propulsion system may be considered as one yielding minimum dry mass. In order to perform the mission, the vehicle required a propulsion system that can operate over the complete speed and altitude range. An RBCC propulsion system with its multiple modes is capable of performing over the required range. The question is whether the RBCC is the correct propulsion system and if it is, how is it designed to maximize performance. Several alternative strategies may be employed in this connection. For example, it may be considered that mission averaged I_{sp} may be improved if, in place of a ducted rocket, a high I_{sp} boost engine is employed, further reducing the amount of onboard oxidizer that must be burned with fuel to accelerate the vehicle to ramjet takeover speed. Alternately, or in addition, airbreathing operation can be extended into the high Mach number scram operation region. Unfortunately, the mass of the resulting conglomerate of engines and decrease in propellant bulk density have a diminishing impact on the vehicle mass fraction that in most cases will more than offset the gains

of higher I_{sp} performance. The system parameters are highly inter-related as can be seen in the following.

2.4.1 Boost Mode Selection

If an engine such as an advanced turbojet or other low-speed airbreathing engine is added, it may appear that improved performance may result. The effective F/m_e ratio of an engine conglomerate is determined by the ratio of the sum of the thrust of the active engines at takeoff divided by the sum of the mass of all engines, active or not. A separate boost-mode engine, used up to, Ramjet Takeover (Mach 2.5), becomes dead mass for the rest of the mission. During boost, such a high I_{sp} boost mode-engine may save 10 mass units of propellant for each mass unit of added engine mass, but to accelerate its greater mass after shutdown to orbit, approximately 4 lbm of propellant per unit engine mass must be burned. After accounting for the added main engine, tank, and thermal protection system masses, the propellant required to accelerate the inactive boost mode engine over the rest of the trajectory significantly exceed the propellant savings during boost. The addition of a boost-mode airbreathing engine also increases the complexity of the vehicle requiring integration of additional ducting with diverters to isolate the boost-mode engine from the high enthalpy flow occurring later in the flight. The associated overall engine development, production, and operation costs are also expected to increase. Since a rocket is needed in the final phase of flight, little weight penalty is experienced with the Ducted Rocket Boost engine. The fully-integrated ducted rocket, yielding a lower vehicle dry weight and a simpler, less costly engine, therefore, becomes the preferred choice for the boost phase.

2.4.2 Engine Design Point Selection

The design of the ram/scram mode is critical since it is the only mode that can add significantly to the mission effective Isp. The thrust produced by an airbreathing engine is directly related to the mass of air processed. This air is captured by the inlet and compressed to raise the pressure for combustion and subsequent expansion. The net accelerating force is the difference between the gross thrust and total vehicle drag (including the spill drag). This total

drag is highest at low speeds when the gross thrust is lowest. When the net accelerating force is low, most of the fuel burned is wasted overcoming the vehicle drag. Higher thrust is necessary to perform the mission. One method is to leave the rockets on longer but this results in much higher propellant consumption. A better method is to increase the airbreathing thrust. The thrust of a ram/scramjet can be expressed in terms of specific impulse $(F/Wdot_f)$, fuel-to-air ratio $(Wdot_f/Wdot_a)$, and the captured air weight flow $Wdot_a$, yielding

$$F = (F/Wdot_f) * (Wdot_f/Wdot_a) * Wdot_a$$

It can be shown that under the conditions that M>5, $(Wdot_f/Wdot_a)$ scheduled to provide minimum fuel requirements for acceleration up to M>10, and flight at constant dynamic pressure the thrust is proportional to the product $Fct(M) * \eta_{cap}$, in which $Fct(M)$ is a function decreasing with increasing Mach number, and η_{cap} is the inlet capture efficiency. Although $Fct(M)$ is to some degree dependent on the efficiency of the overall ram/scram engine design and its integration into the vehicle, the strongest influence on thrust can be materialized through appropriate manipulation of η_{cap}. The inlet capture efficiency depends on the inlet type and the inlet design Mach number. The main determination of the inlet design point is the speed at which the bow shock sweeps back to the cowl lip, a condition referred to as shock-on-lip. Typically, an inlet will achieve full or nearly full capture at its design Mach number. At lower Mach numbers, the inlet will spill increasing amounts of the air. This reduces the thrust produced by the engine and creates spill drag. For a given capture area thrust can only be increased by selecting a lower inlet design point. Figure 14 shows the effect of inlet design point on the capture efficiency. A high η_{cap} at low speeds gives twice the thrust at a time when it is the most needed.

Figure 15 shows the thrust resulting from two different design points. The engine with the Mach 6 design point produces more than twice the thrust of the Mach 12 design at Mach 6, in the middle of the airbreathing acceleration. The thrust does not cross over until after Mach 8, then it is only slightly better than at the Mach 6 design. This higher thrust reduces the drag integral as well as the thermal soak time. The reason that the Mach 12 design outperforms the Mach 6 design above Mach 8 is higher inlet pressure recovery and greater contraction. These are second

order thermodynamic parameters and yield less than 8% improvement in the thrust production. The objective of a space access vehicle is to accelerate the vehicle to orbital velocity and altitude. Only the net thrust, gross thrust minus drag, is providing this acceleration. Net Isp is based on net thrust. Figure 16 illustrates this net Isp as a function of flight Mach number. Figure 17 illustrates the impact of the higher net thrust and Isp on the mission average Isp. The gains in Isp start at the lowest speed with a substantial improvement due solely to the earlier ramjet takeover. The gains continue to improve all the way up to about Mach 8 where the slope of the Mach 6 curve begins to decrease faster than the Mach 12 design. Although performing better at high speed, the Mach 12 design never recovers the large gains made by the Mach 6 design.

The Mach 6 design point engine appears an obvious choice. A critical design issue concerns the ability of the inlet to operate beyond its design point at overspeed conditions. The decline in the thermodynamic efficiency has already been discussed and does not change the design point selection. Typically, this results in the vehicle bow shock falling inside the inlet cowl. If this causes sufficient disruption of the inlet operation, the engine thrust can decrease to a point where it equals the drag. In that case, the higher performance gained at lower speeds is of little use if the engine stops accelerating the vehicle. The inlet designer must build in sufficient overspeed capability into the inlet to permit acceleration past the point of the transition to ascent mode. In Figure 17, it is assumed the Mach 6 inlet can be designed to operate to at least Mach 10.

2.4.3 Ascent Rocket Transition Point Selection

Up to around Mach 15, the a scramjet has higher Isp than a rocket. The issue is at what point is the rising mission average Isp offset by the rising penalties. High Mach number operation increases the thermal loads that must be dealt with. Stagnation temperature increases roughly as the square of the Mach number, requiring more active cooling of the engine and vehicle, and thicker passive thermal protection. Higher speed operation requires a more complex engine with greater variable geometry. These factors add significantly to the vehicle dry weight, and any increase in dry weight requires additional propellant to accelerate the mass. While operating in any pure airbreathing mode, the engine consumes only on-board fuel which, in the

17

case of hydrogen, weighs only 4.5 lbm ft^{-3}. If the scramjet operation is extended beyond Mach 10 more of this low density fuel needs to be stored on-board, increasing the hydrogen fraction and further decreasing the propellant bulk density. The increase in hydrogen usage has also several other negative impacts on vehicle performance. The propellant tank mass is generally proportional to its volume. Low drag hypersonic shape factors produce nonoptimal structural shapes contributing to higher tank mass. The larger tank adds volume and surface to the thermal protection system mass that must be applied to the larger exterior of the vehicle. At the same time the larger frontal area, increased wetted surface, and extended operation in the atmosphere add to the vehicle drag losses. Figure 18 illustrates the effect of airbreathing operation quantified by the choice of transition Mach number on the tanked oxidizer-to-fuel (O/F) ratio and the resulting tank volume for the Strutjet-powered vehicle, assuming that the low speed system is a ducted rocket. It is seen that the tank volume initially decreases due to the increasing I_{sp}. However, as the stored oxygen-to-fuel ratio continues to decrease due to greater airbreathing operation, the fuel tank volume begins to increase. At a Mach number of about 10 and a stored O/F ratio of about 3.0, the minimum dry weight is obtained. Selecting the transition Mach number to be 10 not only reduces the vehicle dry weight but also reduces the engine technology level requirements.

3.0 Strutjet Engine/Vehicle Integration

3.1 Strutjet Reference Mission

An extensive analysis was conducted to determine which launch vehicle configurations have the highest potential for meeting ground takeoff requirements for a launch system delivering 8 klbm to geosynchronous transfer orbit (GTO). An other vehicle was added to this family that would deliver 25 klbm to the international space station(ISS) orbit, proving that Strutjet propulsion offers versatility in overall vehicle design.

Figure 19 shows two options for integrating this type of engine into a vehicle. In the option shown on the left, the Strutjet engine is integrated on the underside of a semi-axisymmetric vehicle. This configuration maximizes the vehicle net thrust value and also

18

provides an efficient structural shape. The figure on the right is a two-dimensional engine configuration.

Of particular interest for two-stage-to-orbit (TSTO) vehicles is the ramjet mode of the Strutjet which enables the vehicle to cruise in the atmosphere like an airplane. This allows omni-azimuthal launching from a single launch site even in the presence of territorial overflight constraints. The vehicle would simply fly in the highly fuel-efficient ramjet mode to a geographical location from where the launch into orbits with inclinations different from the launch site latitude are permitted. This capability also provides the promising prospect of a new, efficiently configured, effectively operated and conveniently located "future spaceport". The cruise mode of operation also provides more flexibility for the return of the reusable first stage vehicle to the launch site after separation of the second stage.

These vehicle studies led to the following conclusions:

- both horizontal and vertical take-off are feasible and practical;

- horizontal landing is required;

- ducted rocket provides good take-off and transition thrust;

- two-stage-to-orbit (TSTO) systems would stage at 16 kft/s, with the first stage returning to launch site;

- single-stage-to-orbit (SSTO) systems are feasible to LEO and ISSO; and

- potential exists for single launch site for all orbital inclinations.

During these studies it was recognized that it is possible to account for the synergistic benefit when the rocket is re-ignited but the vehicle is still in the upper atmosphere. This effect, as stated earlier, amounts to about 5 sec in I_{sp}. Also, the performance of the ascent rocket is critical to the increase in I_{sp}. For example, the mission average I_{sp} is reduced by 4 seconds when the mission ends at the ISSO, instead of LEO, due to the longer operation required in the relatively low performance ascent rocket mode. Some noticeable attributes of the Strutjet can be summarized as follows:

19

- substantially lower takeoff and dry weights than conventional rocket vehicles for all Strutjet-powered vehicles considered

- high dynamic pressure airbreathing operation to only Mach 10

  - manageable aeroheating environments

  - testable with existing facility capabilities

- available material technologies for engine and vehicle

- large potential for future payload growth and cost reductions

  - I_{sp} increase through airbreathing operation at higher than Mach 8

  - mass fraction improvement through advanced materials

  - robustness increase through higher margins and redundancy, and

- single propellant combination for all operation modes, LOX/LH_2.

A typical RBCC vehicle trajectory is shown in Figure 20 compared to an all-rocket vehicle trajectory. The baseline RBCC SSTO-HTHL vehicle flies at constant dynamic pressure of 2000 psf until the transition Mach number is reached. Then, the ascent rocket mode takes over to fly to orbit. The vehicle, having a burnout altitude of about 250,000 ft, is flown into an initial elliptical orbit. The final desired circular orbit is obtained by a Reaction Control System engine (burn phase) to reach low-Earth or higher orbits. For the Ascent/Rocket case, it may be pointed out, the vehicle nominally burns out at about 250,000 ft, and then performs a circularization burn for the final orbit injection. The vehicle masses used here are based on actual vehicle and engine layouts, and simulated flights along trajectories that are optimized either for all-rocket or RBCC propulsion.

3.2 Engine-Vehicle Considerations

Frequently, when comparing propulsion systems. the focus is on the engine characteristics with insufficient attention to the vehicle contribution to the propulsion process. When concentrating on the engine only. its I_{sp} and thrust-to-mass (F/m_e) appear to be the only discriminators between propulsion systems. However, the vehicle stores and provides

20

propellants to the engine. and. in the case of airbreathing engines. it also carries the inlet to supply the ambient air. and provides part of the thrust nozzle. These essential propulsion features have significant impact on the overall vehicle mass and performance. The low bulk density of a hydrogen powered vehicle requires large. heavy tanks. In addition. a Strutjet-powered vehicle flies. when operating in airbreathing modes. more depressed trajectories than typical rocket-powered vehicles in order to ingest the necessary air for propulsion. These factors increase both drag and heat load on the airframe. When comparing propulsion systems one must give full consideration to these vehicle impacts of the propulsion choice.

3.3 Vehicle Pitching Moment

The Strutjet configuration as illustrated in Figure 1 is most effectively integrated on the underside of a vehicle. During atmospheric flight, the fore and aftbody pitching moments caused by the compression of air and the expansion of combustion gases are balanced with vehicle body flaps. Similarly, exoatmospheric control of the pitching moment resulting now only from the expansion of combustion gases can be achieved with a vehicle trailing edge flap as shown in Figure 21. Pitch trim, i.e., net thrust vector directed through vehicle center of mass, can be maintained as the vehicle burns off its ascent mode propellant by deflecting the trailing edge flap by 5 degrees or less. The increase in mass and complexity for the mechanical integration and actuation of the trailing edge flap is less than the incorporation of additional rocket thrusters to control the vehicle during its exoatmospheric operation.

3.4 Engine Performance

The air drawn into the engine by ejector action at subsonic vehicle speeds and by ram effect at higher speeds provides significant (100% and possibly higher) thrust augmentation during boost. The ramjet contribution starting at about Mach 1 increases to full take-over at Mach 2.5. This transition provides the full benefit of ramjet mode of operation with gross I_{sp} values approaching 3800 s. The specific impulses obtained in the ramjet and in the subsequent scramjet mode are shown in Figure 22; these values. which are obtained at a nominal angle of

attack of zero degree and variable geometry of both inlet and nozzle, are corrected for vehicle drag losses corresponding to varying angle of attack during a typical space launch mission.

Figure 23 presents the thrust generated as a function of Mach number for a typical (single) RBCC engine for various operating modes and for a dynamic pressure of 1,500 psf. The capture area is 200 sq. ft. per engine, designed at a shock-on-lip of Mach 6. The net specific impulse generated by the engine is also provided in the previously shown Figure 22, assuming that the rocket is ignited at flight Mach of 10. It is significant to observe here (a) the importance of sizing the engine for transonic flight, (b) the need for high thrust in the vehicle ascent phase, and (c) the effect of the choice of rocket re-ignition Mach number.

3.5 Reduced Operating Cost Through Robustness

It can be shown from several points of view that the Strutjet engine technology leads to lower operating cost for Earth-to-orbit transportation systems. Referring to Figure 24, there are two reasons for this: (i) lower engine replacement cost because the thrust required is reduced to about 70 to 80%, and (ii) lower maintenance and operating cost due to higher structural margins and redundancy. Both of these savings result from the increased I_{sp} of the Strutjet RBCC engine and the associated reduction in take-off and dry masses.

RBCC vehicle design trades that consider engine thrust-to-mass ratio, F/m_e, and transition Mach number M_T are summarized in the previously presented Figure 25 showing the gross mass at ignition as a function of M_T for various values of engine F/m_e. The data show that beyond a M_T of about 10 the vehicle gross mass flattens out. In the generation of these data it is assumed that the thermal protection mass is constant at Mach numbers greater than 10 regardless of the higher heatload experienced. Variations in these two key design parameters, F/m_e and M_T show higher vehicle dry mass for lower M_T and the lower gross takeoff mass for the higher M_T values, even as the F/m_e ratios are lowered.

RBCC SSTO/HTHL vehicle thrust-to-mass ratio and transition Mach number are mapped in Figure 26, and compared to the all-rocket case with a gross takeoff mass of about 2.7M lbm. The

22

engine robustness improvements is given by the point S, with the same dry weight as the all-rocket vehicle but FS equal to 1.68 and F / m_e ratio equal to 25lbm lbm.

The all-rocket dry mass serves in this study as a reference and a design limit. However, in future designs, higher dry mass RBCC vehicles could be considered, as long as robustness and reusability can be further increased and the mission objectives maintained. A prime candidate for further improvement is the thermal protection system.

As noted in Figure 28, the primary structure and propulsion have the largest share of the total dry mass, and adding robustness through mass increase to these elements would have the largest impact on overall dry mass. The landing gear is already designed for mission abort loads, and during routine takeoffs and landings, its design margins are large and no additional robustness is required.

Auxiliary propulsion and other dry mass items make up less than 10% of the total. Robustness increase through redundancy of these items do not have a significant effect on the system dry mass.

The reduced takeoff mass of the Strutjet vehicle, as shown in Figure 30, allows a corresponding reduction in takeoff thrust. Typically, a thrust-to-mass ratios of 1.3 lbf/lbm for vertical and 0.6 lbf/lbm for horizontal takeoff is required to provide adequate vehicle acceleration and "engine out" capability. A reduction in takeoff thrust reduces the required engine size which lowers both replacement, and maintenance and operation cost. Relative to an all-rocket design, a thrust reduction of 80% for the Strutjet baseline, or about 73% for a Strutjet vehicle design with increased structural and engine robustness is possible, as indicated by the point "S" in Figure 30.

Tables 2 and 3 provide, respectively, candidates for engine, and summary of vehicle design features leading to more robustness, but at the cost of increased engine and vehicle mass. Of all the features listed, the powerhead/valving deserves a special comment. The powerhead/valving scheme previously illustrated in Fig. 4 provides the lowest weight system. However, the required mode switching and the various operating conditions of the fuel turbine lead to the surmise that separate turbopumps may represent a more robust approach.

24

To proceed further, the baseline all-rocket and RBCC vehicle designs are compared to the current Space Shuttle launch vehicle in Figure 31. The nominal all-rocket SSTO vehicle is designed with a large forward hydrogen tank, a 15 by 30 ft payload bay, and a single, large rear LOX tank. This arrangement leaves a small trim control margin due to the heavy masses of LOX and engines in the rear. Forward canards may be required, increasing the gross liftoff mass further. The all-rocket SSTO vehicle is about 230 ft., long and the RBCC SSTO vehicle, about 210 ft. The RBCC Strutjet vehicle has two forward and two aft hydrogen tanks, and twin LOX tanks on each side of the payload for optimum center of gravity control. Prior to adding increased "robustness" the RBCC baseline gross mass is about 44%, and the RBCC has a dry mass of about 68% of the all-rocket case.

A layout of a SSTO All-Rocket vehicle is shown in Figure 32. This vehicle is assumed to have 5 rocket engines with 708Klbf thrust each (or 7 engines at 506Klb each) at a F/m_e of 60:1. The vehicle, with a liftoff thrust-to-mass ratio of 1.3, is sized for an abort landing gear with partially loaded propellant tanks. The tanks are designed with a factor of safety of 1.5 using a large graphite-epoxy hydrogen tank, and a single, large aluminum-lithium LOX tank. The mass breakdown for this all-rocket vehicle is provided in Table 4. A layout of a SSTO RBCC vehicle is shown in Figure 33, and its mass breakdown is summarized in Table 5. Comparative design parameters of both vehicles are provided in Table 6.

Both the SSTO all-rocket and the SSTO RBCC vehicle use similar structure and TPS technology, as shown in Figure 34 for the Strutjet vehicle. The TPS is designed for a transition Mach number of 10 and for re-entry thermal conditions. The body structure is graphite-epoxy along with the hydrogen tanks; the LOX tanks are aluminum-lithium; the aerosurfaces are titanium matrix composite (TMC), and the landing gear is titanium. The TPS materials are similar, having carbon-silicon carbide (C-SiC) nose and leading edges, and the polybenzimidezole blanket insulation (PBI) on the top leeward side; Nextel tailored advanced blanket insulation (TABI) or advanced flexible reusable surface insulation (AFRS) is used on the

top leeward side (similar to Shuttle FRSI); and tiles of toughened uni-piece fibrous insulation (TUFI) and alumina-enhanced thermal blanket (AETB) on the reentry lower windward side. The windward side could also have advanced IMI (Internal Multilayer Insulation), but at a much higher cost. The TPS unit mass for the current design over the whole vehicle surface is estimated to be about 1.0 lb/ft^2. This represents a slightly less areal density than current technology (Shuttle is about 1.5 lb/ft^2 average for the whole vehicle).

4.0 Available Hydrocarbon and Hydrogen Test Data and Planned Future Test Activities

The overall test program, accomplished to-date or planned for the near future, may be divided into two groups: (i) missile propulsion tests using storable hydrocarbon fuels, and (ii) space launch propulsion tests using gaseous hydrogen fuel.

4.1 Storable Hydrocarbon System Tests

Aerojet performed a test program which parametrically examined the RBCC Strutjet propulsion system from Mach 0 to 8 over the altitude range from 0 to 100,000 ft. The tests were carried out in the context of a long range missile, two configurations of which are shown in Figures 35 and 36. However, the test results obtained during this campaign are equally applicable to a launch system Strujet like the one described in Section 2. In over 1000 hot fire & inlet tests a number of achievements were realized:

- The strut inlet provides excellent air capture, pressure recovery, and unstart margin.
- The integration of compact high chamber pressure rockets using gelled hypergolic & cryogenic propellants into a strut is structurally and thermally feasible.
- A fixed engine flowpath geometry suitable for all modes of operation can be established providing adequate thrust and specific impulse to accomplish mission objectives.
- Static sea level thrust augmentation of 13% can be achieved due to the interaction of air ingested with the fuel-rich rocket plume.
- The ducted rocket thrust increases with increased flight Math number. At Mach 2.85 and altitude 20,000 ft the thrust increase is over 100%. And, at Mach 3.9 and altitude 40,000 ft. the ramjet thrust exceeds the rocket sea-level thrust by 19%.
- Dual-mode operation of the ram-scram combustor with a thermally choked nozzle is feasible.
- Efficient combustion at high altitude and with short combustors is possible with hypergolic pilots. Combustion efficiency of 90% can be demonstrated with a combustor only 30 in. long at Mach 8 conditions.

Inlet Tests

As part of the first Strutjet inlet test program, a subscale inlet model, shown in Figures 37 and 38,

was constructed to evaluate design options for the freejet engine inlet design. Prior to this testing, engine vehicle performance was based on extrapolating the performance of the inlet from the literature (mostly the work of NASA LaRC). The objectives of the inlet development was to define a missile like inlet that would interface with the hydrocarbon combustor which up to this point had only been tested in a direct connect configuration. A very conservative design was selected that had no internal contraction to assure starting. This inlet was found to start at all tested Mach numbers (4-6), and as shown in Figure 39, it produced excellent pressure rise. As predicted, it exhibited low energy flow near the body side of the flowpath, a phenomenon which had to be dealt with in the subsequent freejet tests via matching the fuel injection with the actual air flow distribution.

Ducted Rocket Tests

In these tests, each strut contained three water-cooled gelled IRFNA and MMH propellant rockets, as shown in Figure 40. The injector pattern consisted of 36 pairs of fuel and oxidizer elements arranged in concentric rings, the outermost ring providing fuel film cooling to the chamber. The chamber geometry is shown in Figure 41. The characteristic parameters of the injector are summarized in Table 7.

As illustrated in Figure 42, the rig representing the Strutjet engine was designed as a sandwich with hinged side wall sections. The duct section housing the strutrocket had a fixed geometry of 4.0 in by 6.6 in. The isolator section in front of the strut duct could be connected to either a bell mouth for a static test or a hydrogen fueled vitiated air heater. Two struts were mounted in the strut duct, dividing the flowpath to the inlet into three channels.

In the sea level static ducted rocket tests the isolator section in front of the strut duct was fitted with a calibrated bell mouth. The duct geometry was varied to determine the configuration yielding the maximum thrust. Sensitivities of rocket chamber pressure, mixture ratio, and rocket nozzle expansion ratio were also established. As shown in Figure 43, thrust enhancement was a strong function of the ram burner throat area and a somewhat weaker function of the ramburner geometry. With a duct geometry of 3°–3°, 13% more thrust was obtained than for the reference rocket in a particular test with a throat area of 32 in^2. Data analysis indicated that oxygen content of the inducted air was completely consumed in approximately 8 in. from the rocket baseline. Considering the influence of chamber pressure, operation at 2000 psia generated more thrust than

28

operation at 1600 psia; however, airflow and thrust augmentation were reduced by 19% and 3%, respectively. The area ratio of 11:1 generated 12% higher induced air flow and 6% more thrust than the lower area ratio of 5:1. Finally, it was observed that greater air flow and higher thrust result from operation at higher mixture ratios due to reduced thermal choking resulting from the afterburning scheme.

In the direct-connect ducted rocket tests which allow evaluation of the engine under flight trajectory conditions, the isolator section in front of the strut duct was connected to a hydrogen vitiated air heater with a Mach 2 nozzle. The duct geometry which, in the static tests, provided the maximum take-off thrust augmentation was maintained in these direct-connect tests. Measuring the duct pressure and assuming a particular inlet performance, allows for the determination of flight altitude and Mach number simulated in a given test.

Figure 44 shows the thrust obtained in the ducted rocket and ramjet tests. The left branch of the figure depicts the thrust of the ducted rocket without additional fuel injection, and the right branch, that of the ramjet without rocket operation. The ducted rocket tests were conducted under fuel-rich conditions, the excess fuel sufficient to support 10 lbm/sec of air flow. The simulated trajectory provides 10 lbm/sec of air at approximately Mach 1.5. Tests beyond Mach 1.5 were thus "lean" on an overall engine stoichiometric basis. Auxiliary fuel injectors could be used to increase the engine thrust. The peak thrust is seen to occur at a simulated altitude of 23,000 ft and Mach 2.85, with 31 lbm/sec of air being supplied to the engine. The peak thrust is over twice the bare rocket value, representing better than 100% thrust augmentation.

Direct Connect Ram and Scramjet Tests

The ramjet tests were conducted at Mach numbers of 2 and higher without rocket operation to optimize ramjet injector performance. The primary ramjet test variable, other than the injector parameters, was the fuel of choice. In support of the strategy for minimizing heat load and hot spots, the main emphasis was on achieving a short combustor length.

In the scramjet operating regime three test series were conducted:

In the first tests the scramjet geometry was explored and high combustion efficiency with a fixed geometry over the Mach number range of 2 to 8 were demonstrated. Mach 2 and 4 tests were conducted with JP-10 fuel. The Mach 8 tests simulated the effect of regeneratively heated fuel

by using ethane instead of JP-10.

In the second test series, the tests conducted with ethane were repeated with JP-10 fuel, using a slightly modified duct geometry, namely the first 12 in. downstream being of constant area followed by a 2° double-sided expansion over the remaining duct length. Auto-ignition was not achieved; however, when pilots were utilized for ignition and flame sustaining, stable combustion at 95% efficiency was observed. As shown in Figure 45, the test duplicated, in essence, the performance previously achieved with ethane, with only the slight change in duct geometry. The Strutjet design used in these tests provided for a contact pilot at each injection point of the hydrocarbon ramjet fuel. This pilot derives its energy from the combustion of small amounts of the gelled rocket propellants which are injected and burned upstream of the hydrocarbon injection. Due to the hypergolic nature of the employed rocket propellants the pilots act initially as igniters and subsequently as flame sustainers, allowing flight at high Mach numbers and high altitudes. The demonstration of this feature is verified by the data presented in Figure 46. At a simulated flight condition of Mach 4 and 40,000 ft of altitude JP-10 was ignited by the pilot resulting immediately in a thrust increase of about 2,000 lbf. Combustion and thrust production were sustained as long as the pilot stayed on. When turned off, the combustion ceases and thrust collapses.

The third test series was in support of the first freejet tests of the Strutjet engine to be conducted by NASA Lewis Research Center at their Hypersonic Test Facility (HTF) in Plum Brook. This facility has the capability to run simulated freejet flight conditions at Mach numbers of 5, 6 and 7 with a dynamic pressure of 1,000 psf. All previous strutjet direct-connect tests, were conducted at a dynamic pressure of 2,000 psf or higher. In addition the Strutjet testing had only been conducted at simulated flight conditions of M = 0-4 and 8. For the sake of risk reduction, additional direct-connect tests were conducted at Mach 6 and 7 at the reduced dynamic pressure. Figure 47 shows the test configuration and also the duct pressures achieved. These tests used the initial combustor divergence found efficient in the ducted rocket/ramjet test series. By properly staging the pilot and the unheated liquid JP-10 injection, good combustion efficiency was achieved without reducing the duct divergence. This was a significant accomplishment since the employed engine geometry proved to be satisfactory for operation from Mach 0 to 8.

Freejet Tests

30

The freejet engine shown in Figure 48 was designed constructed by Aerojet, delivered to and tested at Plum Brook. Tests were conducted with the identical fuel injection strategy used in the Mach 7 direct connect tests discussed above. These tests demonstrated inlet starting, fueled unstart with a large forward fueling split followed by inlet restart with shifting the fuel aft and substantial thrust increase. Figure 49 shows the internal pressure profiles and compares the freejet to the inlet data. Figure 50 shows the differential thrust produced as a function of the fuel flow. The slope break at an equivalence ratio of 0.55 is notable. This is the expected result of the non-uniform airflow distribution in the isolator. In the final test at HTF, the fuel injection distribution was shifted to better match the airflow. Unfortunately the facility experienced a hot isolation valve failure prematurely ending the test campaign.

4.2 Gaseous Hydrogen System Tests

All hydrogen systems considered for the Strutjet engine use cryogenic hydrogen. This hydrogen is used to cool the engine regeneratively. During this cooling process the hydrogen converts from a cryogen to a gas. All combustion related processes of the Strutjet engine will then use gaseous hydrogen as a fuel. Therefore, all combustion related tests were conducted with gaseous hydrogen. The tests described here were executed as part of the Advanced Reusable Technology program sponsored by NASA MSFC and supported by Aerojet with the objective to demonstrate the technology of the hydrogen fueled RBCC Strutjet engine previously described in section 2.

Inlet Tests

The previously shown Figure 4 illustrates schematically the air flow path on the vehicle underbody. Forebody compression reduces the inlet approach Mach number. For example, if the freestream Mach number is 6.0 then the approach Mach number is reduced to 4.2. A model of the inlet-isolator test article is shown in Figure 51. The inlet model accurately simulates the inlet from just upstream of the struts all the way through to the ram combustor. Geometrical similarity between the full-scale SSTO vehicle, capable of delivering 25,000 lbm payload to the International Space Station, and the subscale test article is maintained. The model is 6.8% scale of the full size inlet. The inlet is preceded by a plate simulating the vehicle forebody boundary layer. While the full-scale engine contains 8 to 16 struts and two sidewalls, the test article is composed of two struts and two sidewalls. In the model, the sidewalls are positioned to

31

represent the symmetry plane between struts, thereby fully simulating flow around and between struts. The full-scale engine has two bleed locations, a forebody and a throat bleed. In order to adjust for the non-linear scale effects the inlet subscale model has an additional strut bleed which removes excess boundary layer build up on the sidewalls. A throat plug is used to simulate combustion pressure increase.

The testing of this inlet in the NASA LeRC supersonic wind tunnel provided excellent results. Tests were performed over simulated flight Mach numbers from 3.6 to 8.1. The inlet started at all Mach numbers, and exhibited unstart margins of over 20% in ramjet and 100% in scramjet modes. With forebody spill excluded, engine capture efficiency exceeded 90%, which is remarkable, considering the wide operating range and large unstart margin realized with this inlet. The inlet started easily at all Mach numbers and generated excellent pressure rise, as shown in Figure 52.

Strut Rocket Tests

Aerojet and NASA Marshall Space Flight Center completed proof-of-concept testing on a new strut rocket injector element developed to enable operations under the unique strutrocket conditions. This element has been incorporated into the design of six subscale strut rockets for ducted rocket testing.

The primary objective for a part of these tests was to demonstrate the performance and durability of a new injector which had been designed to maximize thruster efficiency while minimizing thruster length. The injector design ensures efficient mixing of the propellants within the chamber by employing an impinging element design and by utilizing a refined element pattern: 18 elements on the 0.5 inch diameter injector face. Figure 53 shows the injector firing in a single chamber in tests at Aerojet. Thermocouple data verified that the temperature of the injector face was within the limits predicted for the design. Post-test visual inspections of the test articles indicate that the injectors suffered virtually no erosive or other damage related to excessive face temperatures. Scanning electron microscope images of single elements and single orifices produced at MSFC are particularly encouraging. The data obtained during 16 hot-fire tests extend over the ranges indicated in Table 8:

Subscale strutrockets were fabricated and check out tests were complete. In these tests the propellant, coolant and ignition sequences required for RBCC operation were developed, and

32

unaugmented rocket thrust was determined to establish a reference for subsequent combined cycle testing. Aerojet is also currently fabricating a full scale strutrocket using the same injector element. During the testing of this test article laser diagnostics will be used to measure the fuel distribution in the rocket exhaust for various design and operating conditions.

Direct Connect Ram & Scramjet Tests

Aerojet successfully demonstrated the efficiency of this fuel injection strategy at Mach 6 and 8. Figure 54 shows one of the test strut assembly for the direct connect campaign. Two struts are shown installed in the test rig in Figure 55.

Three test series were conducted: ram and scram tests at simulated Mach 6 flight conditions, and scram mode tests at Mach 8 conditions. High performance was achieved in all three test series in only 27 tests. A key to this success was the use of the cascade scram injectors in the forward location. The fuel split for each mode and Mach number was determined by the inlet tolerance to the combustion pressure rise. Excellent performance at stoichiometric conditions was demonstrated at each Mach number and mode tested, by simple adjustment of the fuel flow to each of the three injectors. The data indicated that the performance of the cascade injector was even better than expected. Evidence of over-penetration suggested additional improvement can be made by increasing the number of cascades from 4 per strut side to 5 or more. This can be expected to increase the combustion rate and permit even shorter, lighter engine designs.

Planned Tests

In the first two tests strutrockets, shown in Figure 56, will be installed in the direct connect duct to explore the performance in the Scram/Rocket and Ascent/Rocket Modes.

A second pair of strutrockets will be installed in the new freejet engine and tested first under sea level static conditions and then in the ducted rocket and ramjet modes. Of particular interest is the transition from ducted rocket to ramjet mode at a flight Mach number of about 2.5. An external view of the freefet test hardware is shown in Figure 57. To accommodate aerodynamic flow conditions inside the freejet test facility, the test hardware nozzle flap shown in Figure 3 is integrated on the body side of the engine; in the flight engine the nozzle flap will be on the opposing cowl side.

The contemplated test facility has the capability to provide accelerating test conditions. This allows tests to begin at one Mach number and sweep continuously to a higher one while simultaneously matching pressure and enthalpy. Using this facility, it will be possible to demonstrate the ducted rocket to ramjet and the ram to scram transitions.

4.3 Planned Flight Tests

The development of a Strutjet powered vehicle poses challenges above and beyond that of classical rocket vehicles. The most significant difference is that for RBCC propulsion vehicle an engine must be developed simultaneously with the flight vehicle. Flight demonstrations are essential, since simulated flight conditions are costly or not at all obtainable on the ground. In order to reduce the development risk of such vehicles, it is proposed to advance the technology readiness levels incrementally using two demonstration vehicles and engines as defined in Tables 9 and 10. With a length of about 35 ft the first test vehicle, TV-1 is about 1/16th scale relative to the full scale SSTO vehicle previously presented in Fig. 33.

Test Vehicle TV-1. A typical, small 35-ft RBCC X-plane is shown in Figure 58. Its dry mass is about 24K lbm. This vehicle could be air launched from a B-52, or ground launched to test out all RBCC engine operating modes. The air-launched vehicle is sized for a maximum burnout Mach number of 10. A small payload bay (2X4 ft) is available for instrumentation. The configuration layout is similar to the full-scale SSTO vehicle. There are two RBCC engines, each having a sea-level thrust of 9.8Klbf, for a total ignition thrust of 19.6Klbf.

The two trajectories for the X-plane flights from a B-52 at 40Kft altitude and ground launch are compared in Figure 59. The air-launched mission profile is flown at a maximum dynamic pressure of 1500 psf, and achieves a burnout Mach number of about 10 at about 100Kft altitude. In contrast, the ground launched mission profile is flown at a maximum dynamic pressure of 2000 psf, and achieves a burnout Mach number of about 7.8 at 83Kft altitude. These two trajectories were computed using the OTIS ("OPTIMAL TRAJECTORIES by IMPLICIT SIMULATION") code developed by The Boeing Company.

The engines required for this 35 ft vehicle will focus on thrust, specific impulse performance and controller characteristics. They will be light weight, however, due to their small size the demonstration of thrust-to-mass ratio and life capability are not the objective of these tests. Control functions to be developed involve variable geometry for inlet and nozzle, inlet bleed valve control, and rocket and ram-scram propellant flow control.

Test Vehicle TV-2. This vehicle can be similar in length to the full-scale SSTO vehicle previously shown in Figure 32, except it will only be powered by one full size Strutjet engine with 346Klbf of thrust which allows the vehicle to be about 40% narrower from tip-to-tip. Since the purpose of this vehicle is to demonstrate reusability and low maintenance operation it will be structurally very similar to the final vehicle.

5.0 Maturity of Required Strutjet Technologies

The maturity of RBCC engines is best defined in terms of a 'Technology Readyness Level" (TRL) as defined by NASA. The following assessment is as of Summer 1998 relative to a TRL of 6 which requires technology demonstration in a relevant environment be it simulated on the ground or actually flown. Table 11 categorizes various aspects of an RBCC engine into the degree of maturity relative to TRL 6.

It is evident from the table that a large amount of development must be accomplished before a TRL of 6 is achieved for the Strutjet RBCC engine. With this assessment in mind, it may not be prudent to risk at this point in time the commitment of large amount of resources towards the exclusive RBCC approach to achieve low cost access to space. Alternate approaches, like further maturation of all rocket propulsion, should be employed. However, the potential of RBCC engines is so overwhelming that it is also not prudent to casually dismiss the opportunity to exploit this option.

6.0 Summary and Conclusions

Strutjet propulsion has the potential to provide substantial engine "robustness" design margins over an all-rocket system. These design margins can be used to reduce operating cost through reduced maintenance activities of the highly reusable system and the reduction in engine replacement cost possible through a significantly smaller vehicle and horizontal takeoff. Using advanced technologies the achievable thrust-to-mass ratio of the engine is about 35 lbf/lbm. Making use of the available "robustness' design margin, this number can be reduced to about 23 lbf/lbm. Runway takeoff provides a reliable pre-airborne propulsion health verification coupled with an operational attractive abort mode.

An Strutjet powered SSTO HTHL design has the potential to also offer structural "robustness" design margins over an all-rocket SSTO VTHL vehicle. Results show that, prior to adding robustness, the RBCC vehicle gross takeoff mass is about 44 percent of the all-rocket case, and the RBCC vehicle dry mass is about 68 percent of the all-rocket case. Adding structural "robustness" to the RBCC vehicle, by for example increasing the factor of safety from 1.5 to 1.68 and using an engine with a thrust-to-mass ratio of 25 lbf/lbm, the resulting dry mass does not exceed that of an all-rocket vehicle. The gross take-off mass (1.7M lbm) increases to only about 63 percent of the all-rocket level (2.7Mlbm) while keeping the transition Mach number at 10. Since the required thrust-to-mass ratio of the Strutjet HTHL vehicle is only 0.6 versus the corresponding ratio of 1.3 for the all-rocket vehicle, the Strutjet vehicle with its increased robustness benefits from a thrust reduction of 73%.

If the all-rocket vehicle landing system were designed for a total lift-off abort mass with fully-loaded tanks, even greater "robustness" could be built into the RBCC vehicle before dry mass equivalence is reached. Also, the RBCC robustness design margins would increase slightly for higher transition Mach numbers and higher engine thrust-to-mass ratios, provided that no added cooling requirements are needed for the TPS subsystems. Therefore, the RBCC vehicle design has added structure and engine "robustness" design margins available to become equivalent to an all-rocket vehicle's total dry mass under the same design ground rules.

Hydrogen And Hydrocarbon Strutjet Engines - These engines, particular the hydrogen fueled

one, have made considerable progress, and test data established to date verify their fundamental feasibility and support earlier performance predictions. While the current NASA Advanced Reusable Technology (ART) Program as well as Aerojet sponsored test activities will provide additional data during 1998 and early 1999, no further design or test activities are currently planned for storable hydrocarbon RBCC engines.

Strutjet Technology Maturity - Although significant achievements have been made towards a Technology readiness Level of 6, demonstration in a relevant environment, most of the effort to date is focused on flowpath development and performance assessment. Future work must be done on engine structure, thermal management, and propellant feed system. Ground tests of flight type engines are mandatory before committing these advanced engines to in-flight, captive carry or self-powered, evaluation.

Overall Recommendation

It has been shown that Strutjet propulsion with its superior robustness has the potential to reduce maintenance, operations and engine replacement cost. However, at this point in time, no specific cost figures are obtainable because of the unavailability of sufficiently refined engine and vehicle designs, the lack of detailed maintenance procedures and operational scenario definitions, and above all, the absence of a representative, generally accepted operational cost model. Current models use the vehicle dry mass as the figure of merit for cost operating cost determinations. For the RBCC case, this would be invalid, because the RBCC system with its intentionally increased dry mass is substantially more operations cost effective than the reference all-rocket system with equal mass. The establishment of a representative and credible cost model is needed before the cost benefits of robust RBCC propulsion can be quantified.

7.0 References

1. W.J.D. Escher and B.J. Flornes (Dr. Murthy to complete)
2. F. Billig and D. Van Wie (Dr. Murthy to complete)
3. classical ejector ramjet concepts (Mel Bulman to complete)
4. US Patent No.5.220.787 "Scramjet Injector", issued to Aerojet June 22.1993

Table 1:

Parameter	Rocket	Strutjet	Reduction
Chamber Pressure	3000 psia	2000 psia	33%
Fuel Pump			
Discharge Pressure	7000 psi	3000 psi	57%
Turbine Inlet	1700 ^{0}R	1000 ^{0}R	41%
Temperature	2000 rpm	1700 rpm	15%
Turbine Tip Speed	100%	72%	28%
Rotational Stress			

Table 2:

Feature Providing Engine Robustness	Sensitivity To Engine Robustness Increase
General	
Engine Thrust-To-Mass	High
Reduced Transition Mach Number	High
Specific	
Redundant Ignition	Low
Health Monitoring	Low
TPA Housing Stiffness	Medium
Reduced Turbine Speeds/Temperature	Medium
Reduced Chamber Pressure	Medium
Separate Fuel TPA's Ducted Rocket Mode Ram/Scram & Unducted Rocket Modes	High

Table 3:

Design Approach	Nominal Condition		Growth Level Potential	Impact on Robustness/ System
o Increased Tank Factor of Safety (FS)	1.5	→	>2.0	High (Lifetime)
o Choice of Materials	Al LO_2 Gr/Ep LH_2 Gr/Gp Str.	→	Develop New Materials	Med (Cost)
o Materials Physical Properties (Tanks)	Al = 80 ksi Gr/Ep = 75 ksi	→	+25–50%	High (Lifetime,Handling, Maintenance)
o Design Margins	0	→	+25%	Med (Lifetime)
o Handling	Min Gauge 0.100–0.200	→	X2.0	High (Maintenance)
o Fabrication and Design	Optimum Thickness	→	Thicker Skins and Web Isogrid	Med (Lifetime, Handling)

Table 4:

- $F/m_o = 1.3$ lbf/lbm @ liftoff

MODULE	COMPONENT	Mass (lbm)	Mass (lbm)
1.0	Forward Nose	3,347	
2.0	LH₂ Tanks – Intertank	27,773	
3.0	LO₂ Tanks – Intertank	15,021	
4.0	Cargo Airframe	11,062	
5.0	Wing/Tail/Structure	16,776	
6.0	Boattail Structure	2,969	
	● Total Primary Structure		76,948
7.0	Landing System	24,093	
8.0	Electrical/Mechanical/Actuation	5,450	
9.0	Thermal Protection (TPS)	26,633	
10.0	Avionics/Environment	2,263	
11.0	Power	567	
	●		135,954
12.0	OMS/RCS (Dry)	4,346	
13.0	Main Propulsion (Dry)	81,640	(F/m$_e$=60 lbf/lbm)
	● Total Vehicle Dry		221,940
14.0	Residuals/Reserves/He	39,644	
15.0	Propellants (Main, OMS, RCS)	2,395,398	
	● Total Liquids		2,435,042
	● Total Vehicle (No P/L)		2,656,982
	● Payload		25,000 (ISS)
	● Total Ignition		2,681,982

Table 5:

- $M_r = 10.0$
- $T/m = 0.6$ lbf/lbm @ liftoff

MODULE	COMPONENT	Mass (lbm)	Mass (lbm)
1.0	Forward Nose	2,477	
2.0	LH$_2$ Tanks + Intertank	25,089	
3.0	LO$_2$ Tanks + Intertank	7,509	
4.0	Cargo Airframe	7,015	
5.0	Wing/Tail/Structure	11,388	
6.0	Boattail Structure	3,456	
•	Total Primary Structure		56,933
7.0	Landing System	34,896	
8.0	Electrical/Mechanical/ Actuation	5,450	
9.0	Thermal Protection (TPS)	18,174	
10.0	Avionics/Environment	2,263	
11.0	Power	567	
•	Total Dry (Less Prop)		118,283
12.0	OMS/RCS (Dry)	3,690	
13.0	Main Propulsion (Dry)	33,166	(RBCC F/m$_e$=35:1)
•	Total Vehicle Dry		151,449
14.0	Residuals/Reserves/He	19,692	
15.0	Propellants (Main, OMS, RCS)	972,061	(m$_{runway}$ = 44,629 lbm
•	Total Liquids		991,753
•	Total Vehicle (No P/L)		1,143,202
•	Payload		25,000 (ISS)
•	Total Ignition		1,168,202

Table 6:

Parameter Vehicle	All-Rocket	Strutjet RBCC
Vehicle Length	230 ft	210 ft
Wing Span (Tip-To-Tip)	110 ft	94 ft
Number Thrust Per Engine	5 @ 708K lbf Or 7 @ 506K lbf	2 @ 346K lbf
Engine Thrust-To-Mass	60 lbf/lbm	35 lbf/lbm
Lift-Off Thrust-To-Mass Ratio	1.3 lbf/lbm	0.6 lbf/lbm
Tanks - Operating Pressure - Factor Of Safety - Number/Material LH$_2$ Tank - Number/Material LO$_2$ Tank	45 psi 1.5 1 ea Graphite/Epoxy 1 ea Aluminum-Lithium	45 psi 1.5 4 ea Graphite/Epoxy 2 ea Aluminum-Lithium
Oxidizer To Fuel Loading Ratio	6.0 : 1	3.4 : 1
Runway Propellant	None	45K lbm
Propellant Ullage	3%	3%
Propellant Residuals	1% for the main 3% for the OMS/RCS	1% for the main 3% for the OMS/RCS
Vacuum Specific Impulse For All Onboard Propulsion Systems	450 sec	450 sec
Vehicle Prime Structure Mass	77K lbm	57K lbm
Total Dry (Less Propulsion) Mass	136K lbm	118K lbm
Total Vehicle Dry Mass	222K lbm	151K lbm
Total Useable Propellants	2,365K lbm	951K lbm
Usefull Mass Fraction	0.8992	0.8461
Landing Gear Mass	1% Of Mass @ Ignition Note: Vehicle does not reach ISS orbit with higher landing gear mass	3% Of Mass @ Ignition
Mass @ Ignition	2.682K lbm	1,168K lbm
Robustness Margin	Reference: 0K lbm	71K lbm
Thrust Reduction	Reference: 0%	80% prior to, 70% after robustness increase to no robustness margin

Table 7:

Parameter	Design	Nominal Operation
Mixture Ratio	1.6	1.4
Chamber Pressure (psia)	2,500	1600–2000
Thrust (lbf)	1,000	600–700
Expansion Ratio	5.1 and 11.1	5.1 and 11.1

Table 8:

Chamber Pressure (psia)	Mixture Ratio	Test Duration (sec)
100 – 1800	4.76 – 7.0	1 – 5

Table 9:

Attribute	Test Vehicle: TV - 1	Test Vehicle: TV - 2
Airframe Demo Objective	• Propulsion and vehicle system technology testbed • Vehicle system development • Mid/high speed controllability • Propulsion integration	• Flight-weight engine • Flight-weight structure • All vehicle systems • Aircraft-like operations
Length	• Small Scale (30-40 ft)	• Large Scale (~ 200 ft)
Speed Range	• Ground Launched: M = 0 -7.8 • Air Dropped Launched: M = 0.8 -10.0	• M = 0 -10.0
Vehicle Structure	• Inexpensive • Robust • Advanced materials and structures	• Flight-weight materials and structures
Thermal Protection	• Robust baseline TPS • Actively cooled leading edges and inlet ramps	• Active and passive light-weight TPS
Demonstrations	• Cryogenic tankage and propellant feed system • Power generation • Actuation Systems • Avionics	• All flight-weight systems • Redundancy • Reliability/maintainability

Table 10:

Attribute	Test Engine: TE - 1	Test Engine: TE - 2
Propulsion Demo Objective	- Performance - All Modes All Transitions - Flightweight Structure - Controllability Operability	- Performance - All Modes, All Transitions - Flightweight Structure - Controllability Operability - Reliability Maintainability
Rocket Propellants	LOX LH2	LOX LH2
Ram Scram Propellants	LH2	LH2
Engine Structure	- Lightweight - Inexpensive - Composite Structure - Advanced Materials	Flightweight Materials And Structure
Engine Thermal Mgmt - Rocket - Leading Edge/ Inlet Duct - Ram Combustor	- Water Cooled - Uncooled - Water Cooled	- Hydrogen Cooled - Hydrogen Cooled - Hydrogen Cooled
Powerhead - Ox Preburner - Ox TPA - Fu PB - Rocket Fu TPA - Ram/Scram Fu TPA	- Modified Existing Design - New Subscale Design using ball bearings - Modified IPD Design - New Subscale Design using ball bearings - New Subscale Design using ball bearings	New Full Scale Design using hydrostatic bearings
Other Subsystems	- Bread Board Controller - Existing Flight Type Valves - Electro Magnetic Valve & VG Actuation - Instrumentation as required	All components reflect high degree of life and robustness - Reliability - Maintainability

Table 11:

Top Level Technology Item	Sub Tier Technology Item	Degree of Technology Maturity		
		Low	Medium	High
Flowpath Integration	Design Point Selection		x	
	Balanced Performance Along Flowpath		x	
Fuel Injection	Penetration, Mixing, Vaporization		x	
	Stable Combustion		x	
	Controlled Heat release		x	
Light Weight Structure	High Temperature Materials			x
	Radiation Cooled Structures	x		
	Regeneratively Cooled Structures	x		
	Endothermic Fuel Reactions		x	
	Closed Loop Cooling	x		
Strut Rockets	High Thrust-To-Mass			x
	Long Life		x	
Turbo Pumps	Low Weight	x		
	Long Life Bearings		x	
	Low Temperature Turbines		x	
	Multi Mode Operation	x		
Engine Controls	For All Flight Modes	x		
Testing	Ground Test Subscale		x	
	Ground test Full Scale	x		
	Captive Flight Of Engine Module	x		
	Self-Powered Flight Of Flight Type Engine	x		

Vehicle

Ram Combustor

Nozzle Flap

Isolator
Scram Combustor

Cowl

Ram Injectors

Variable Geometry
Scram Injectors

Inlet Strut

Combustor Struts

Nozzle

Ram Combustor

Strut Rockets

Isolator

Scram Combustor

Wind Screens

Forebody

Figure 1

Strut Rockets

Strut Inlet

Figure 2

Figure 3

Flight Mode 1.a

Legend
O₂
Burned O₂ Rich
Burned H₂ Rich
H₂

Air

Mode	Cycle	
	O₂	H₂
1. a. Ducted Rocket	PB	GG
b. Ducted Rocket	PB	GG
c. Ducted Rocket	PB	Exp
2. Ramjet	Off	Exp
3. Scramjet	Off	Exp
4. Scramjet/Rocket	PB	Exp
5. Unducted Rocket	PB	Exp

Rocket Flow | Ramjet Fuel Flow | | | Geometry | |
Base | Aft | Fwd | Inlet | Nozzle

Figure 4

Figure 5

Flight Mode 1 Mach 10+
Oxidizer Preburner & H2 Expander

Strut Rocket: Pc=1000 psi
Scramjet: On

Legend

O2 — Burned O2 Rich — Burned H2 Rich — H2

Turbine

FGGIBTV
FGGBTV

FGG

FGGOTV
FGGFTV

Pump
FRV

LH2

FSV

MFV

STRUT ROCKET

BASE AXIAL
FTEV1

RAM
FTEV2

ENGINE COOLING

ORV

LOX

OSV

Pump

OPBOTV
OPBFTV

OPB

FEMTV
FGGTV

SCRAM
FTEV3

Turbine

Figure 6

Figure 7

Figure 8

Bypass Ratio Wair/Wrocket

Isp - sec

Thermal Choking Reduces Air Induction

All Burnt

Rayleigh Loss Included
Design Bypass = 2 (W/O Afterburning)

% Initial Air Burned

0   1.0   1.5

Hydrogen Burned (% of Rocket Flow)

Rocket Thrusters
4 per Strut

Base Axial Injector
3 per Strut

Vehicle Side

Cowl Side

Ram & Scram Injectors

Air Flow Channels

Strut

Figure 10

Rocket Plume Core

Turbine Plume
• Embedded In
Rocket Nozzle

Rear View

Turbine Plume
• Entrained Into Rocket Plume

Ejector Pumping
Limited Heat Release

Afterburning
Turb. Gases Exposed
to Pressurized Air

Distance From Rocket Exit Plane

Figure 11

Strutless Engine

Airflow → Products

Fuel, Fuel, Fuel

Combustion

Wall Injectors :7

Combustor Length = 60 G

Mixing Gap G

Front View

Top View

Strut Engine

Airflow → Products

○ Shorter Combustor
○ Reduced Combustor Losses
○ Reduced Heat Load
○ Higher Thrust
○ Higher Isp

Struts: 3
Injectors : 30

Combustor Length = 60g

Reduced Mixing Gap g

Figure 12

Cascade Injector   Conventional Injector

Figure 13

Flight Mach Number

Figure 14

Figure 15

Figure 16

Stage Effective Isp

Estimated Mach 6 Design Over Speed Limit

Strong Influence of
RJ Takeover Mach

Md = 6

Md = 12

2   4   6   8   10   12   14

Transition Mach Number

Figure 17

Tank Volume Increases Above Mach 8

Figure 18

Reentry Side

Propulsion Side

270°

Semi-Axisymmetric Concept

2-D Lifting Body Concept

Figure 19

Figure 20

Flap Angle δ

Trailing Edge Flap

Nozzle Length, 100%

Desired Net Thrust Vector In
Exoatmospheric Rocket

Cowl Extension, 10%

CG

Figure 21

Figure 22

Why Strutjet
For Access
To Space?

Mission Average Specific Impulse
Increased By 40%

30% Vehicle Dry Mass Margin
Allows For Robustness Increase

• Increased Vehicle Safety Margins
• Thrust - To - Engine Mass: 23 instead of 35lbf/lbm
• Full Subsystem Redundancy

Lower Maintenance/Operating
Cost

Allows For Horizontal Takeoff

70-80% Reduced Takeoff
Thrust

* Lower Engine Replacement Cost
* Pre-Takeoff Runway Checkout
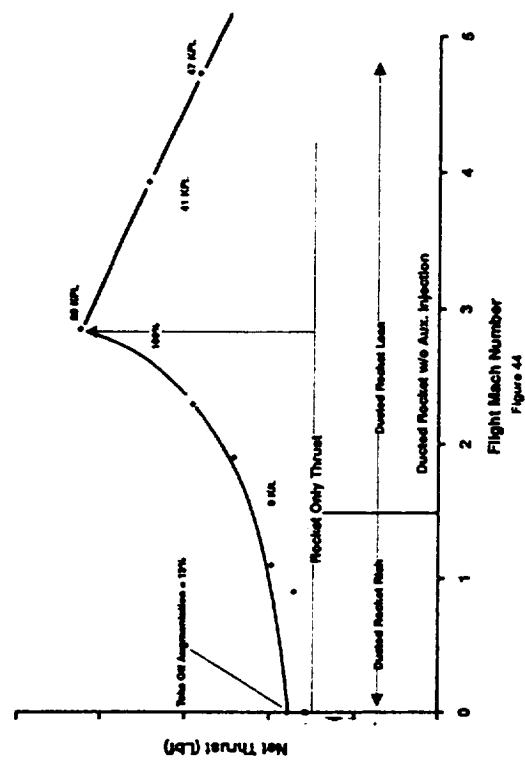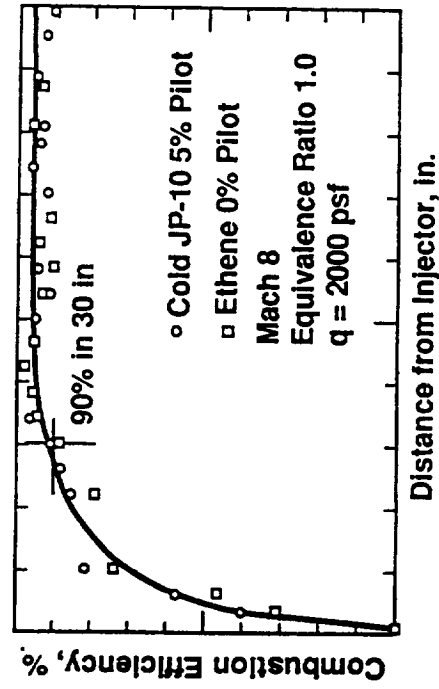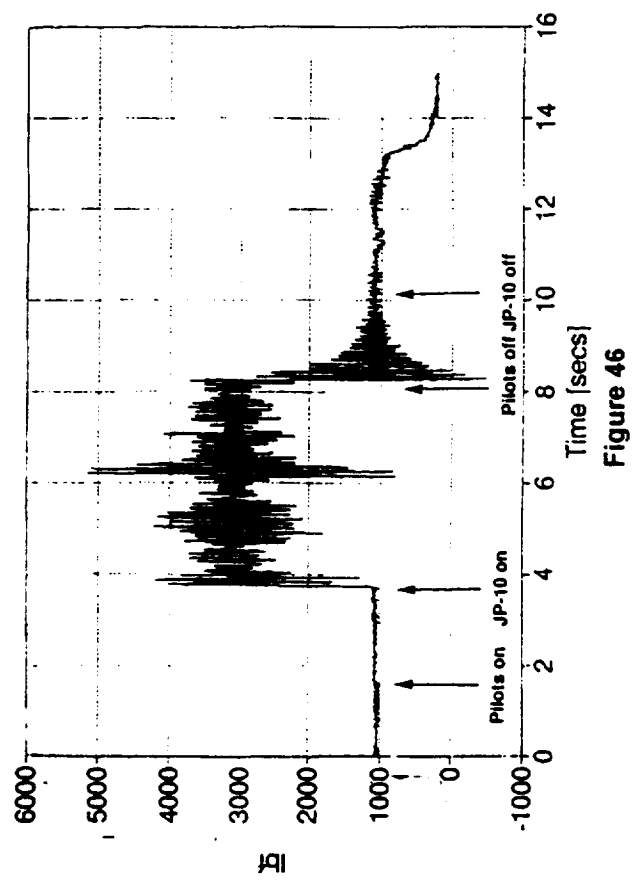* Safe Abort

Strutjet Lowers
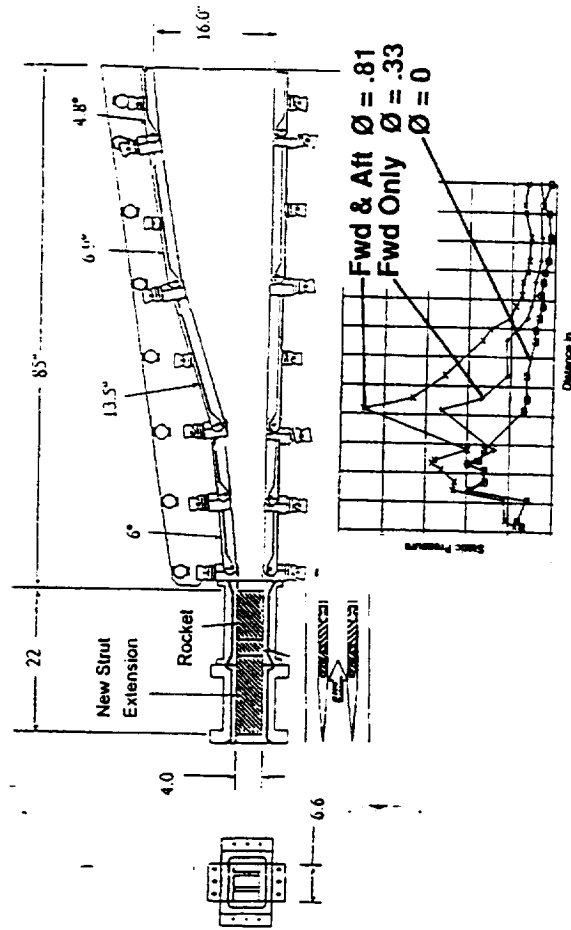Access To Space
Cost!

Figure 24

Figure 25

Figure 26
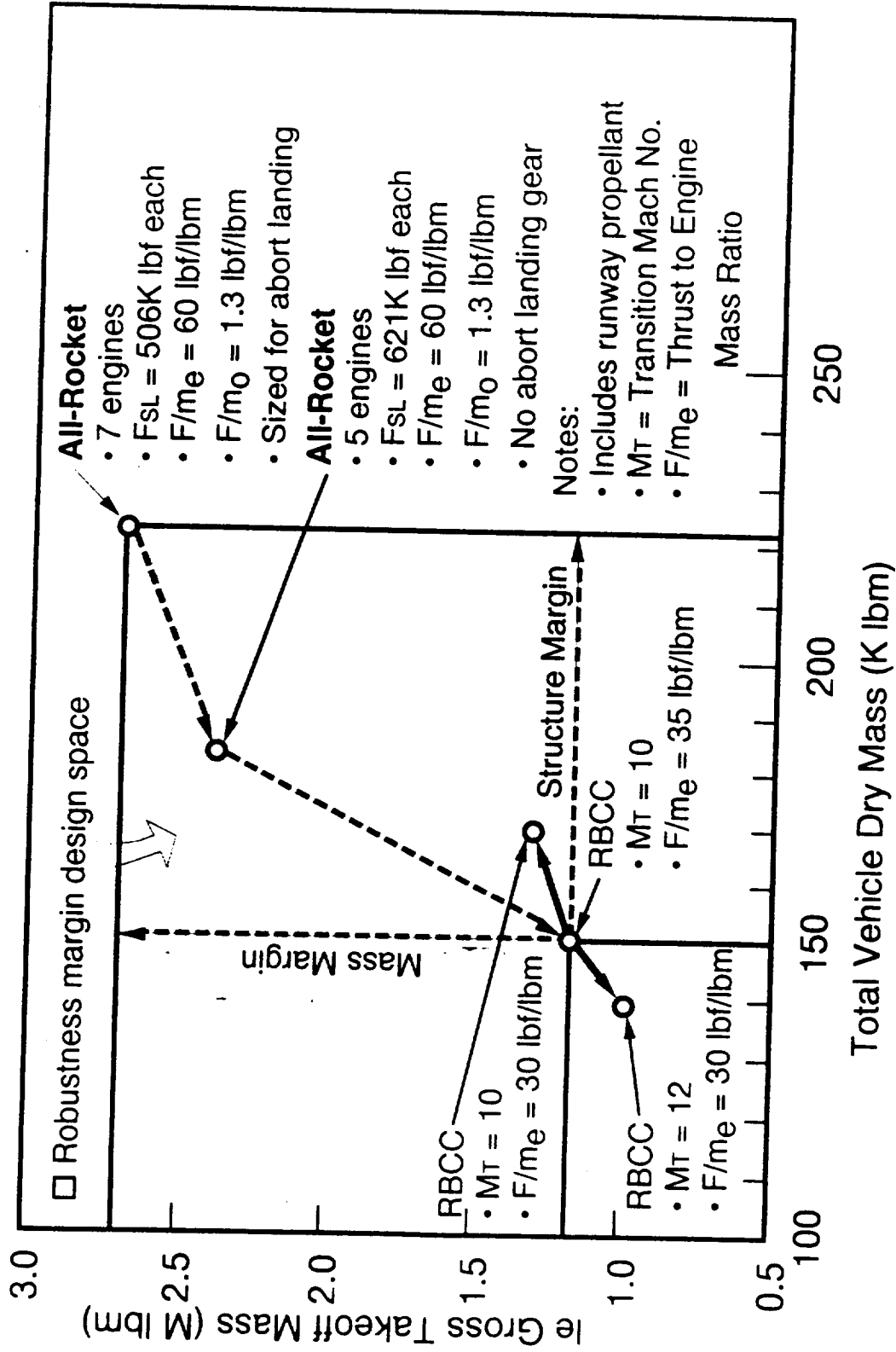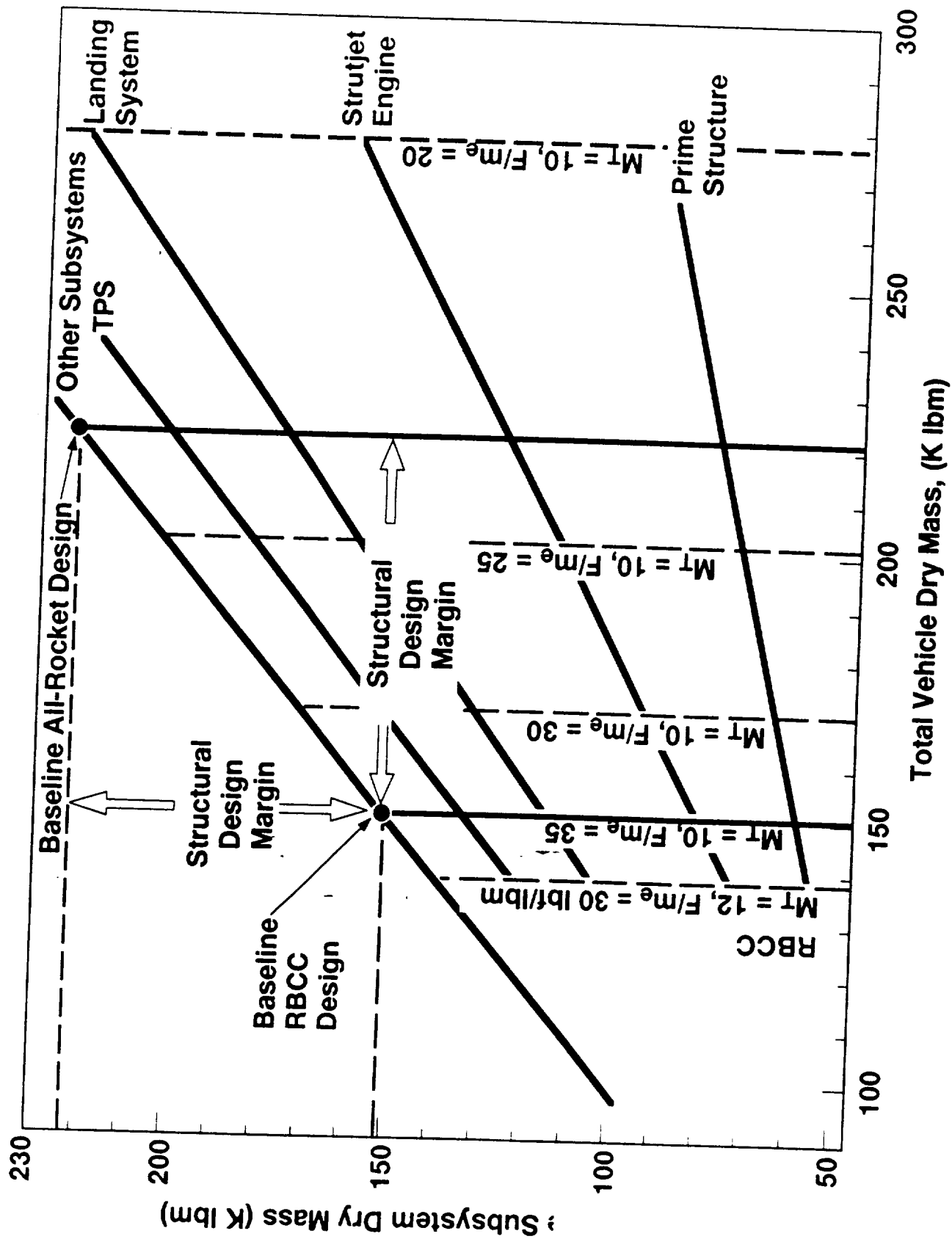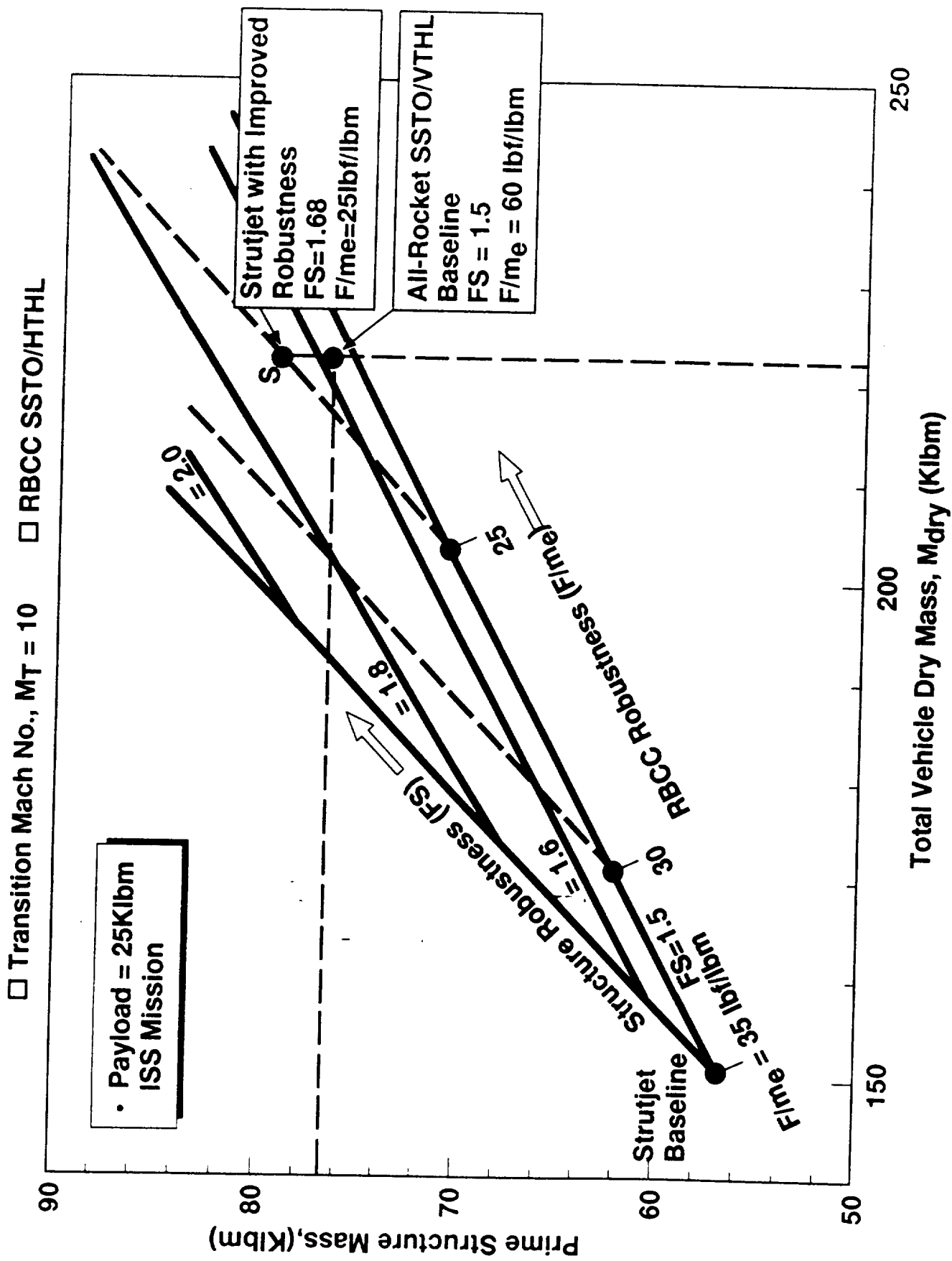
Figure 27

Figure 28

Figure 29

Figure 30

Figure 31

Payload Bay 15 x 30 ft

Vehicle	Shuttle	SSTO/VTHL	SSTO/HTHL
Propulsion	Rocket	Rocket	RBCC
Takeoff Mass (Mlbm)	4.5	2.7	1.2
Dry Mass (Klbm)	508	222	151

System Length (ft)

250 200 150 100 50 0
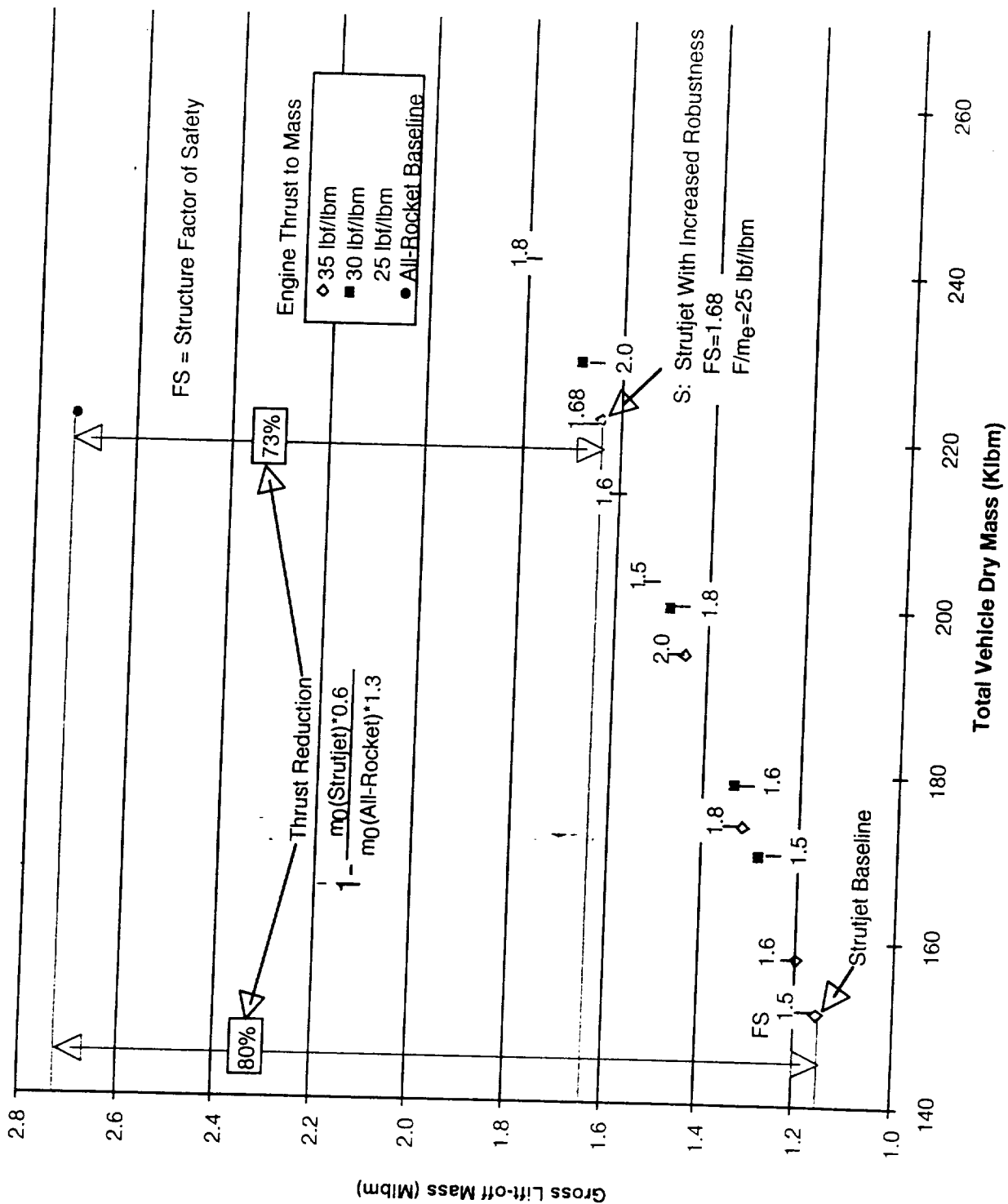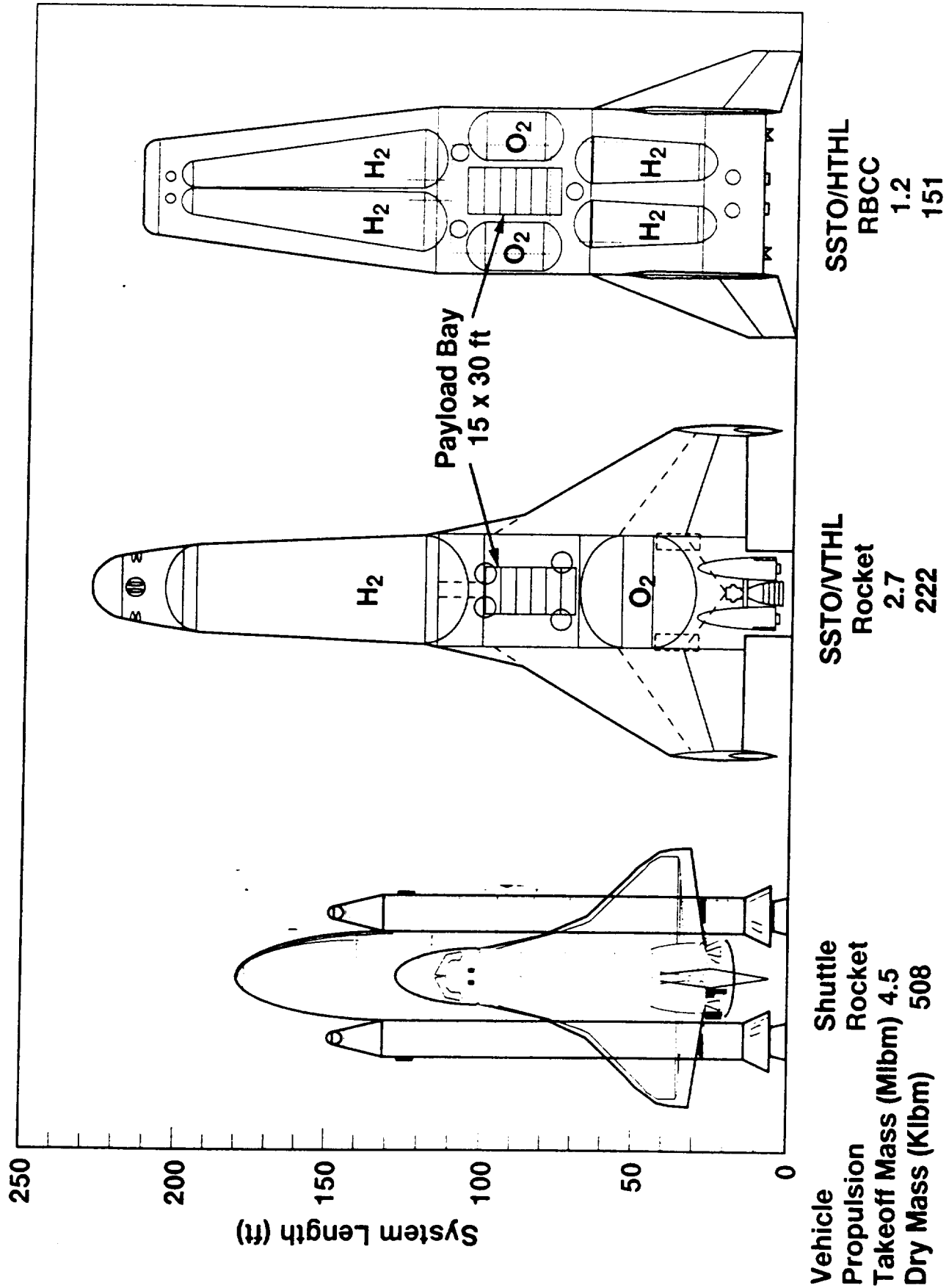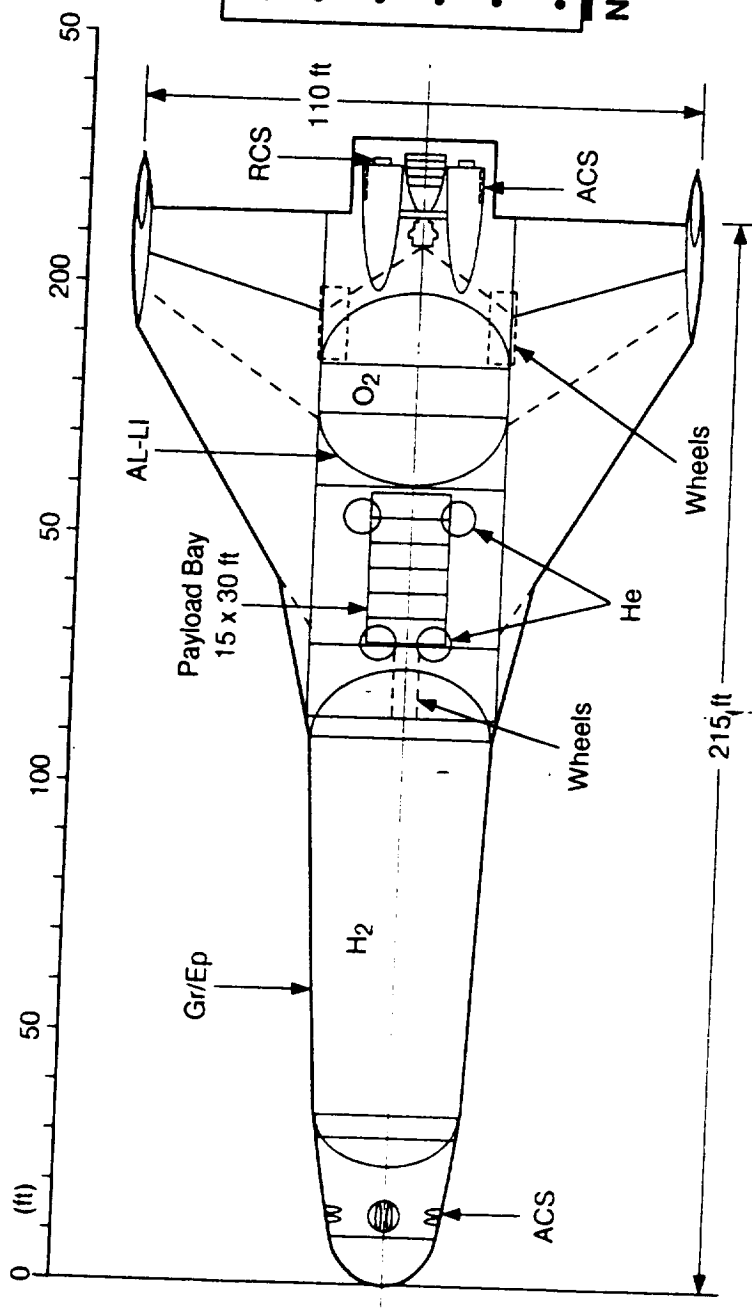
- ISS P/L = 25K lbm
- m_0 = 2,682K lbm
- m_p use = 2,365K lbm
- m_{dry} = 222K lbm
- F/m_e = 60 lbf/lbm
- F/m_0 = 1.3 lbf/lbm

Note: **Landing gear sized for abort**

$5 \times 708K$ lbf
F/m_e = 60 lbf/lbm
I_{sp_V} = 450 sec
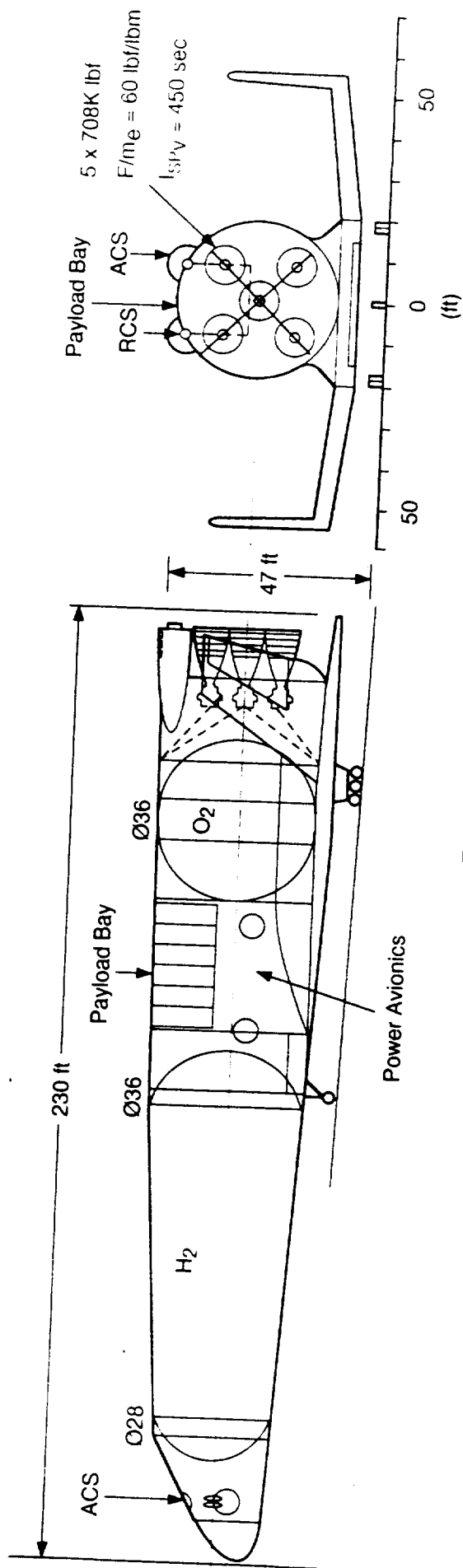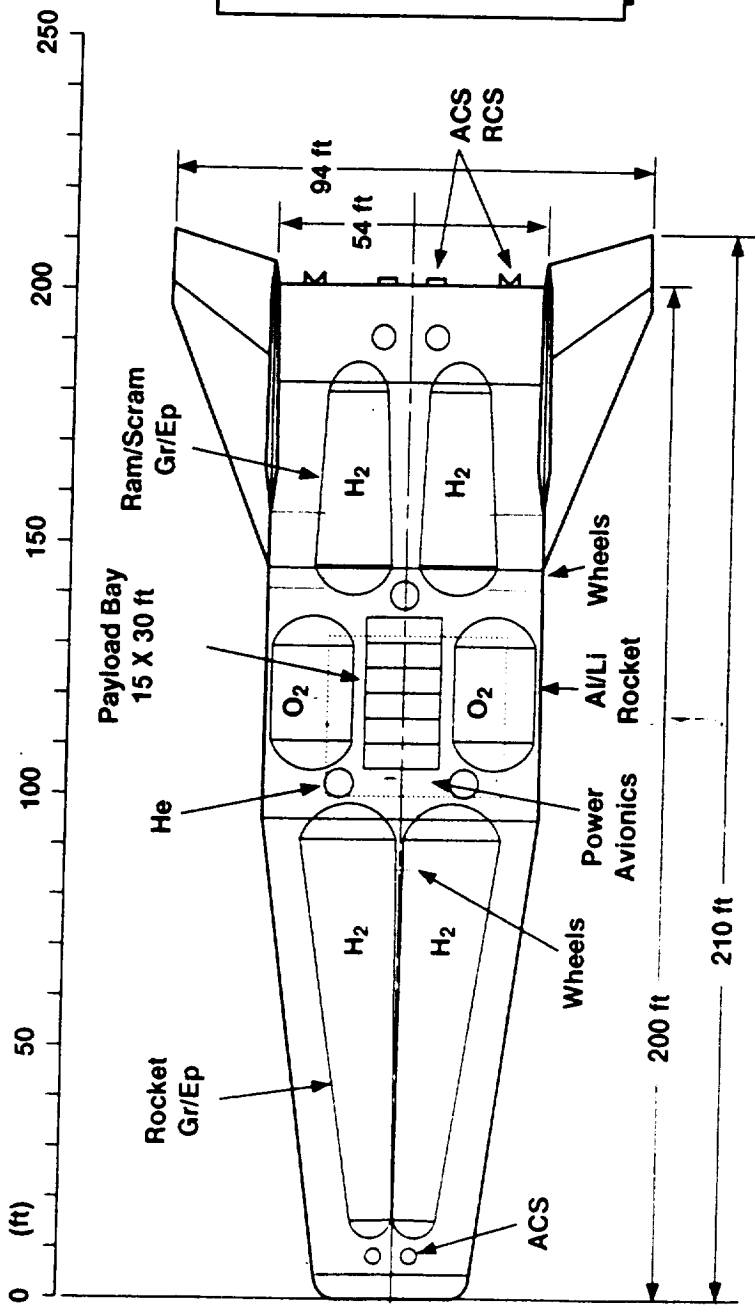
Figure 32

- ISS P/L = 25K lbm
- Transition Mach No. = 10
- m_0 = 1197K lbm [1]
- m_p use = 951K lbm
- m_{dry} = 151Klbm
- F/m_e = 35 lbf/lbm
- F/m_0 = 0.6 lbf/lbm

(1) Runway Propellant
     Included (45K lbm)
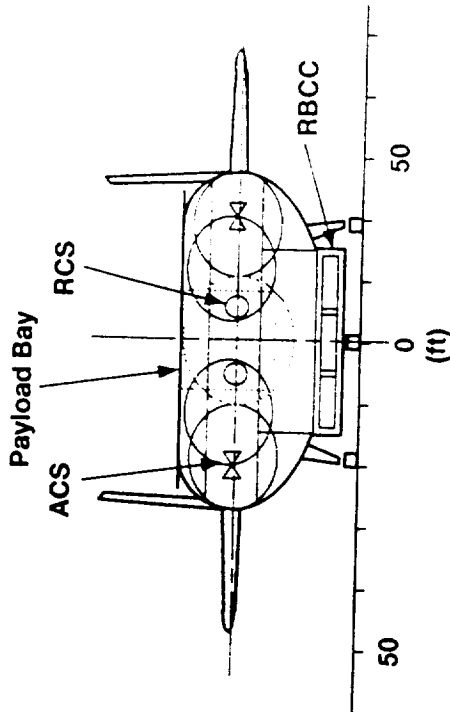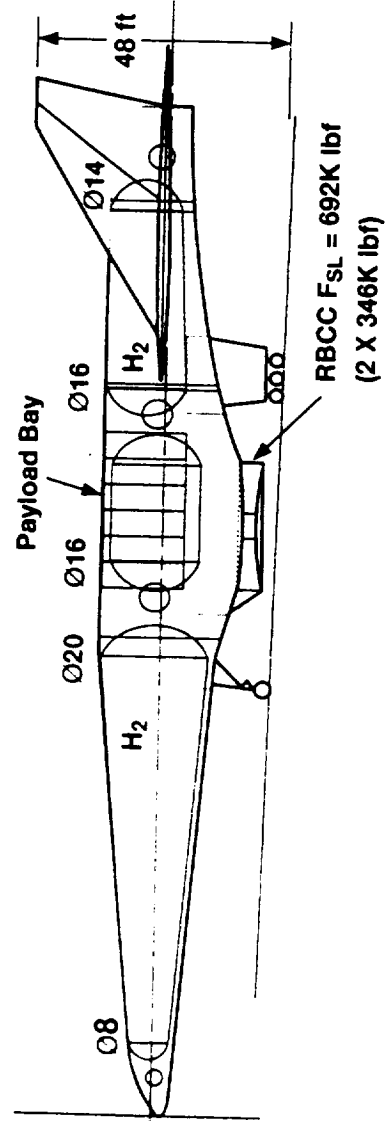
Figure 33
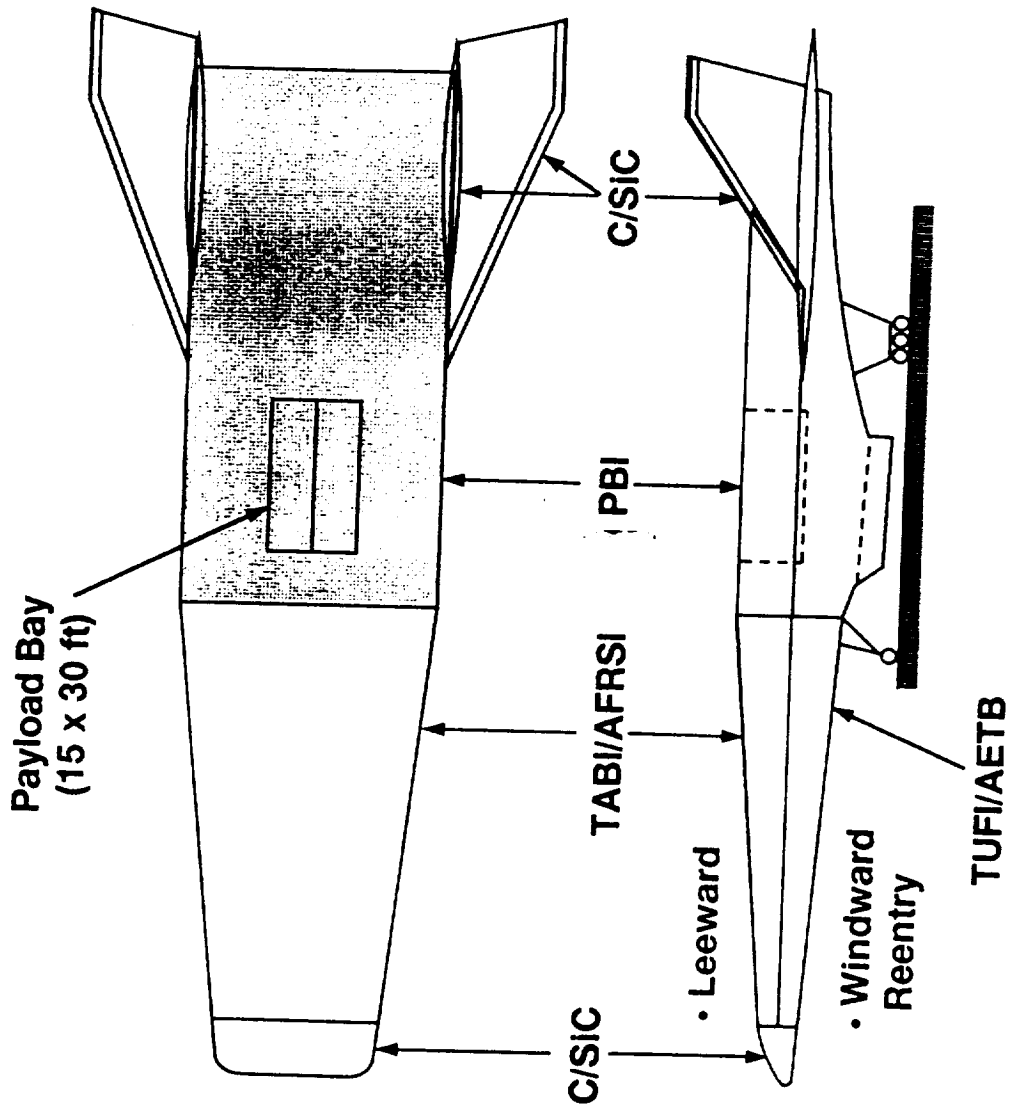
■ **Structure** — **Materials**

1. Body — Gr/Ep
2. H₂ Tanks — Gr/Ep
3. O₂ Tanks — Al-Li
4. Aero Surfaces — TMC
5. Landing Gear — Ti

■ **Primary Structure (lbm) = 56,933**

■ **TPS** — **Materials**

1. Nose/Leading Edges — C/SiC
2. Leeward/Top Rear — PBI
3. Leeward/Top Front — TABI/AFRSI
4. Windward — TUFI/AETB

■ **TPS Mass (lbm) = 18,174**

Payload Bay
(15 x 30 ft)

C/SiC

C/SiC

PBI

TABI/AFRSI

• Leeward

• Windward
Reentry

TUFI/AETB

■ **Mass at Ignition = 1,168K lbm**

Figure 35

Scram Position

Ram Position

Variable Nozzle

Ram Burner

Scram Burner

Warhead& Avionics

Propellants

Seeker

Strut Rockets

JP-10 Injectors

Windscreens
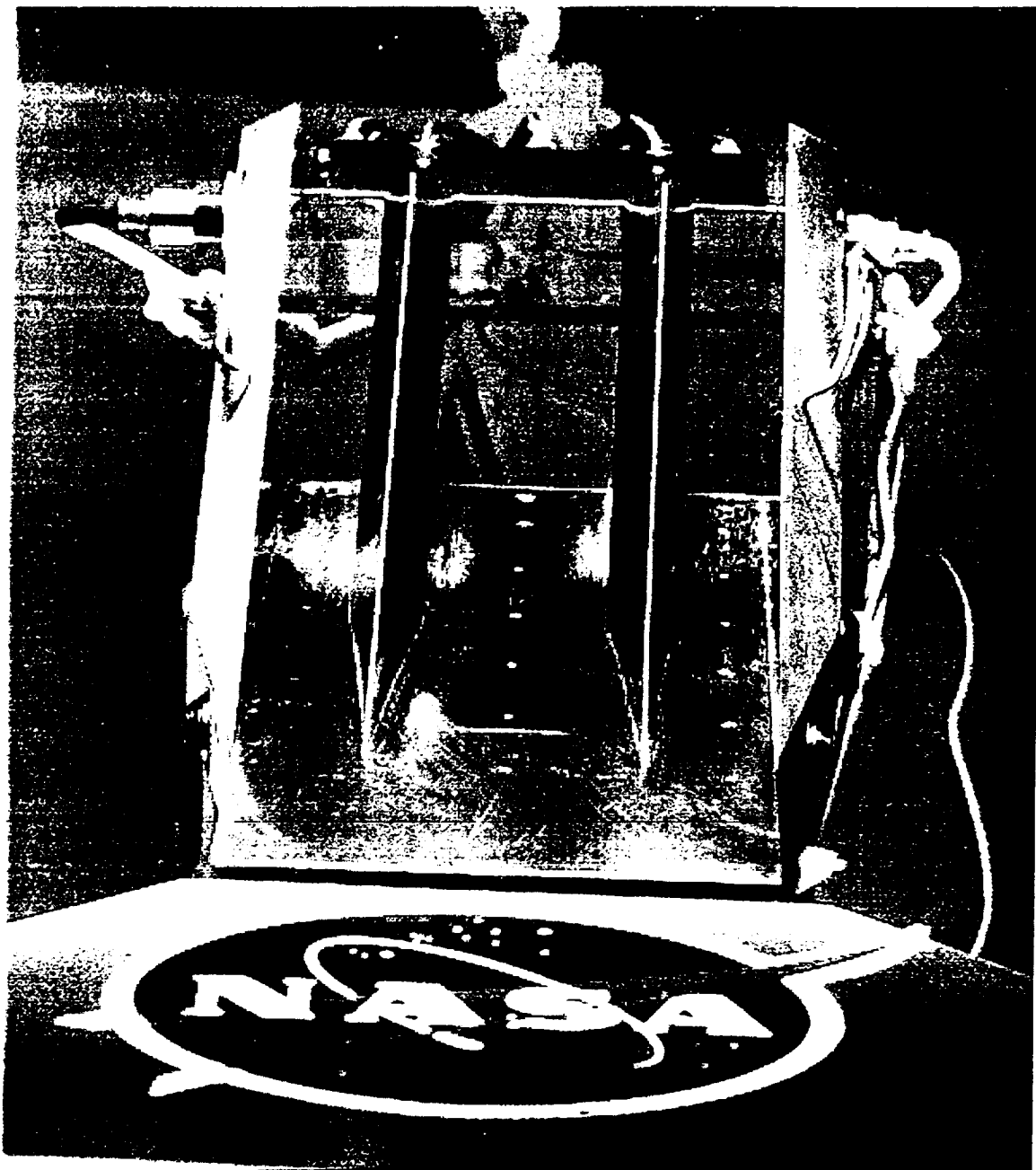
Spike Inlet with Strut Compression
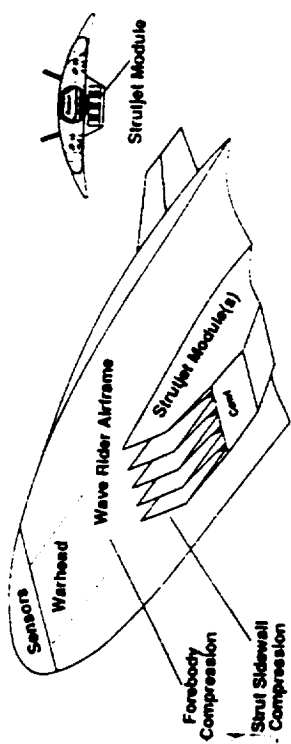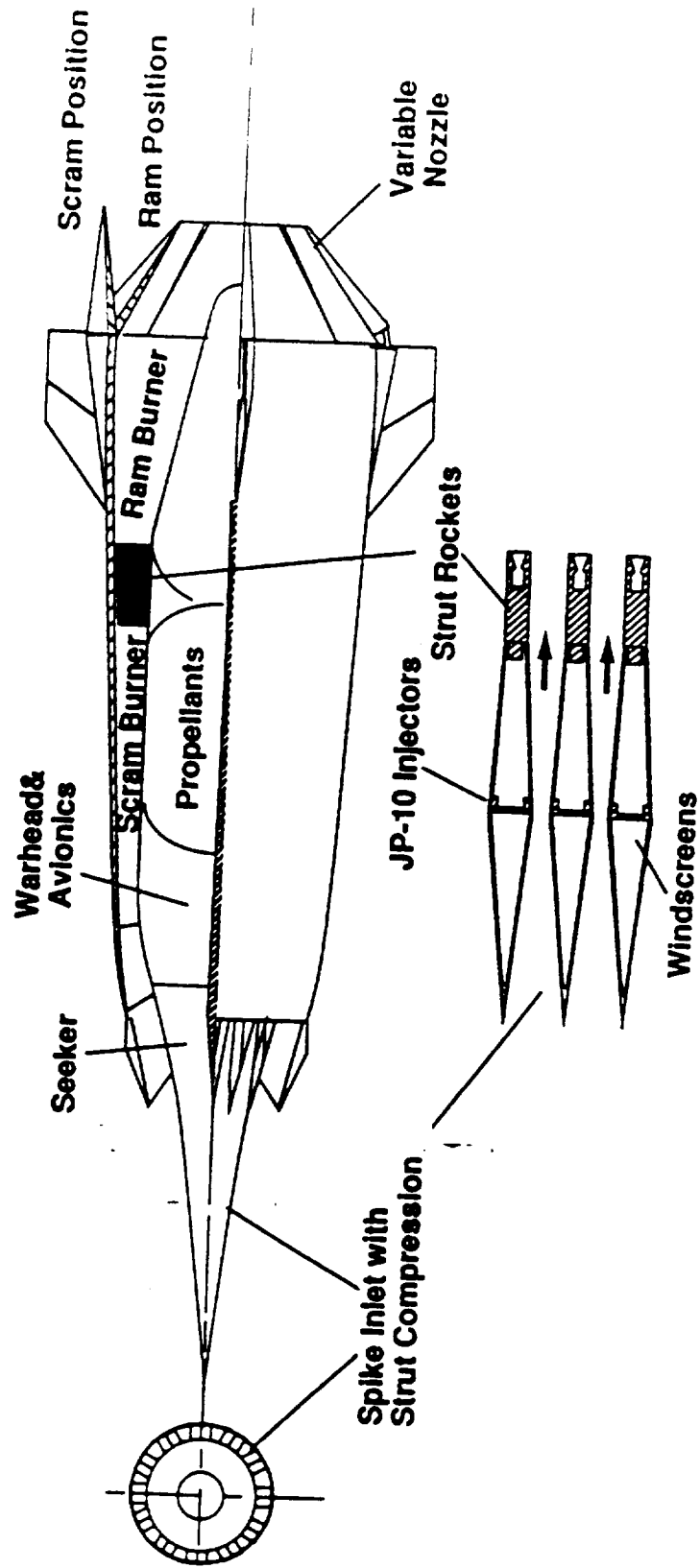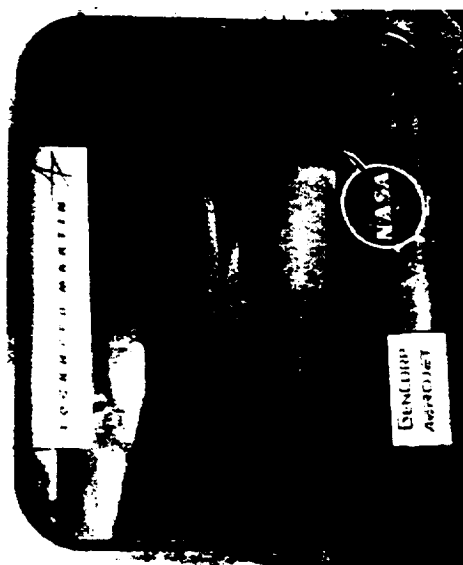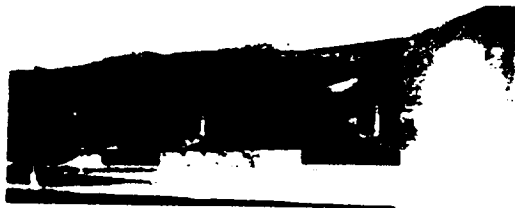
Figure 36

Figure 37

Figure 38
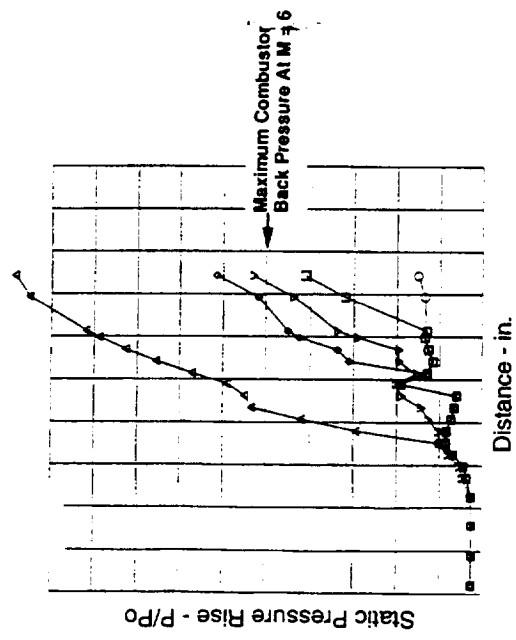
Figure 39

Fig 39
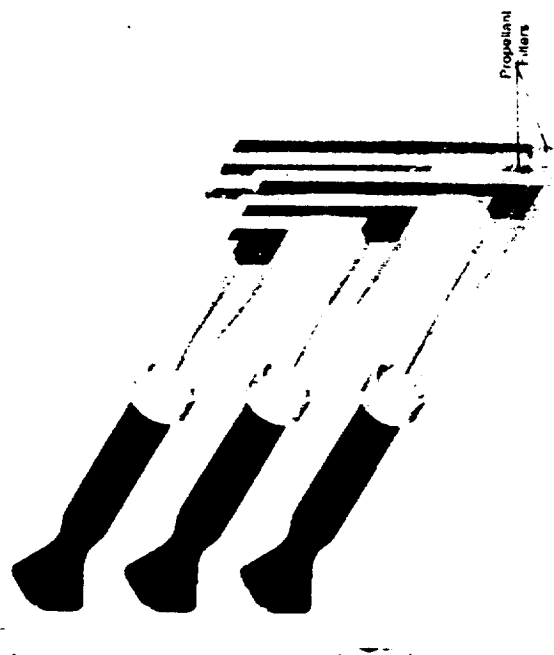
Figure 40

Figure 41
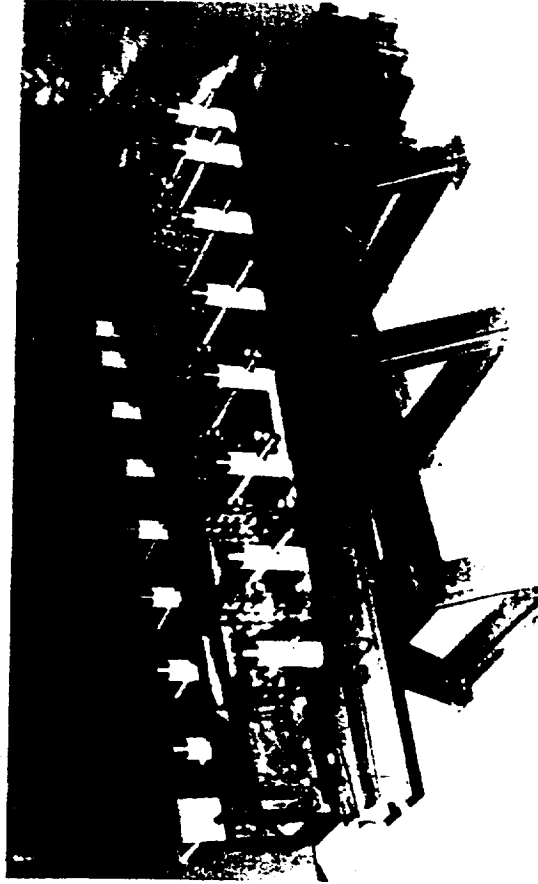
Figure 42
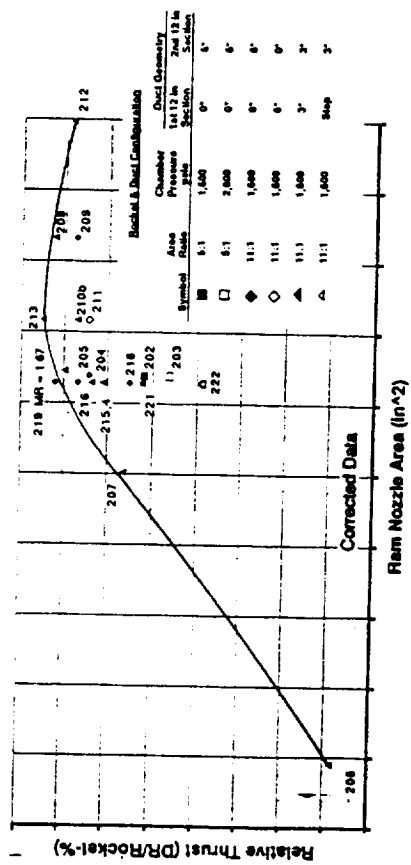
Figure 43

Flight Mach Number
Figure 44

Figure 45

Figure 46

Figure 47

Figure 48

Figure 19

Legend:
- Tare, Unfueled
- Supersonic Combustion
- With Back Pressure

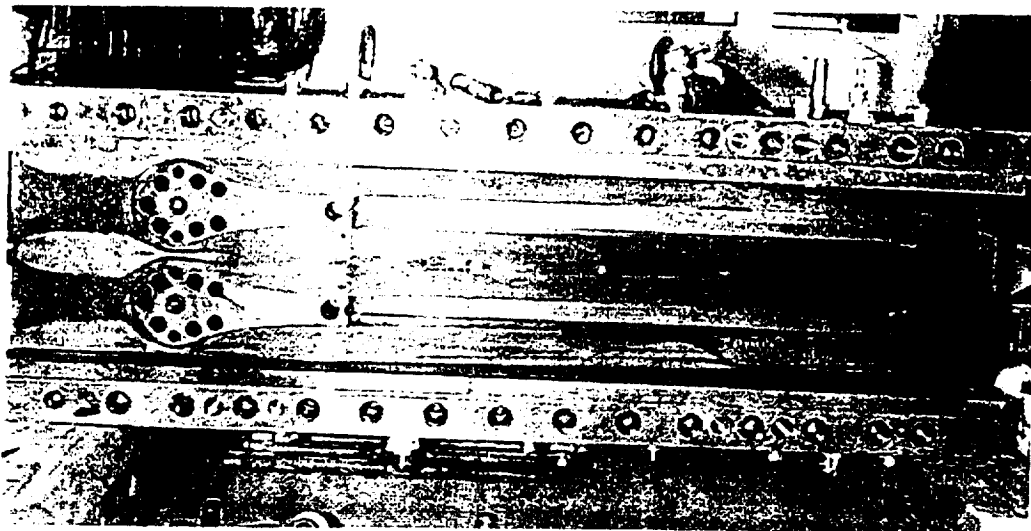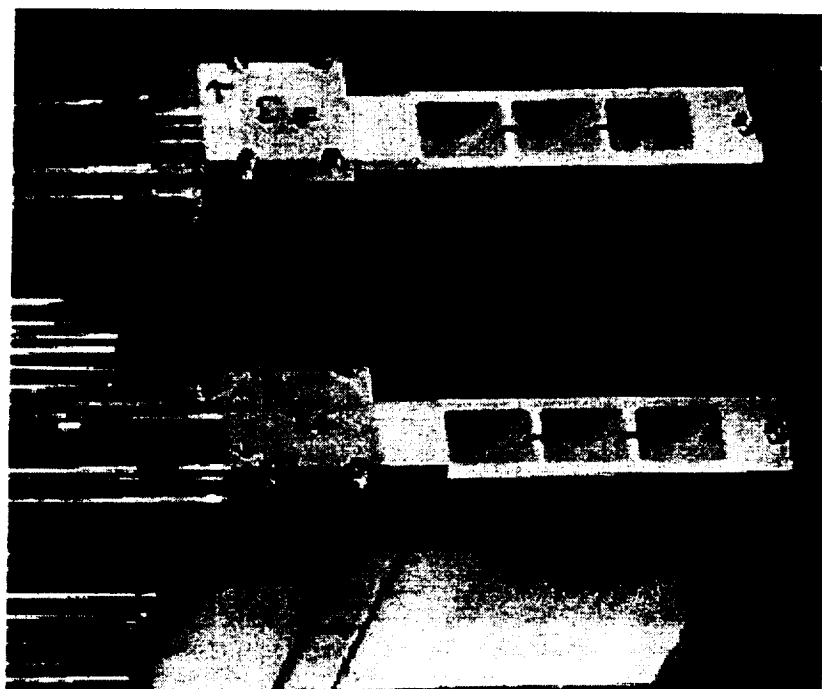x (in)

Ps/Pso
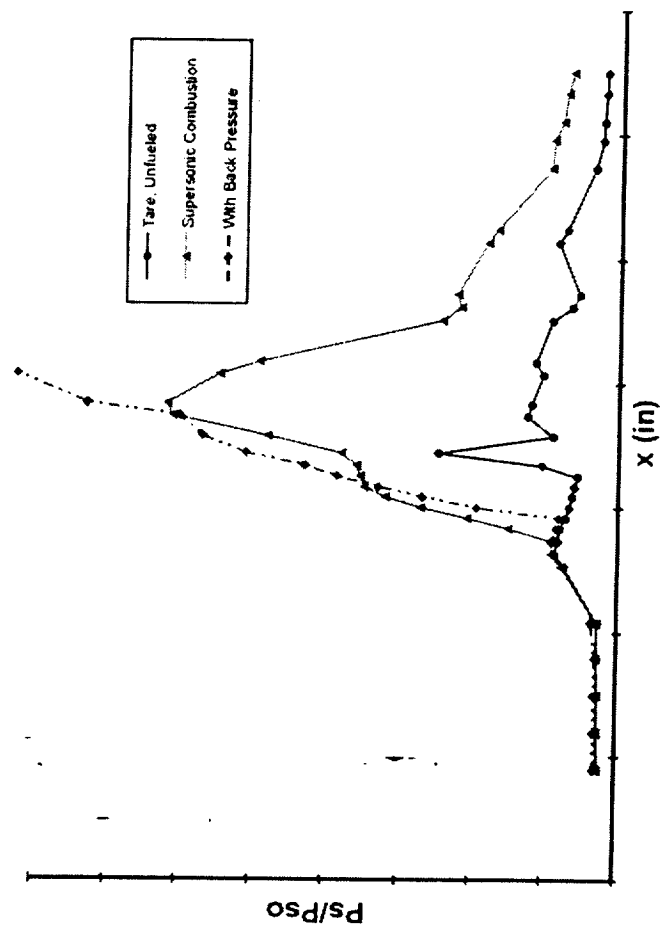
Fig 49
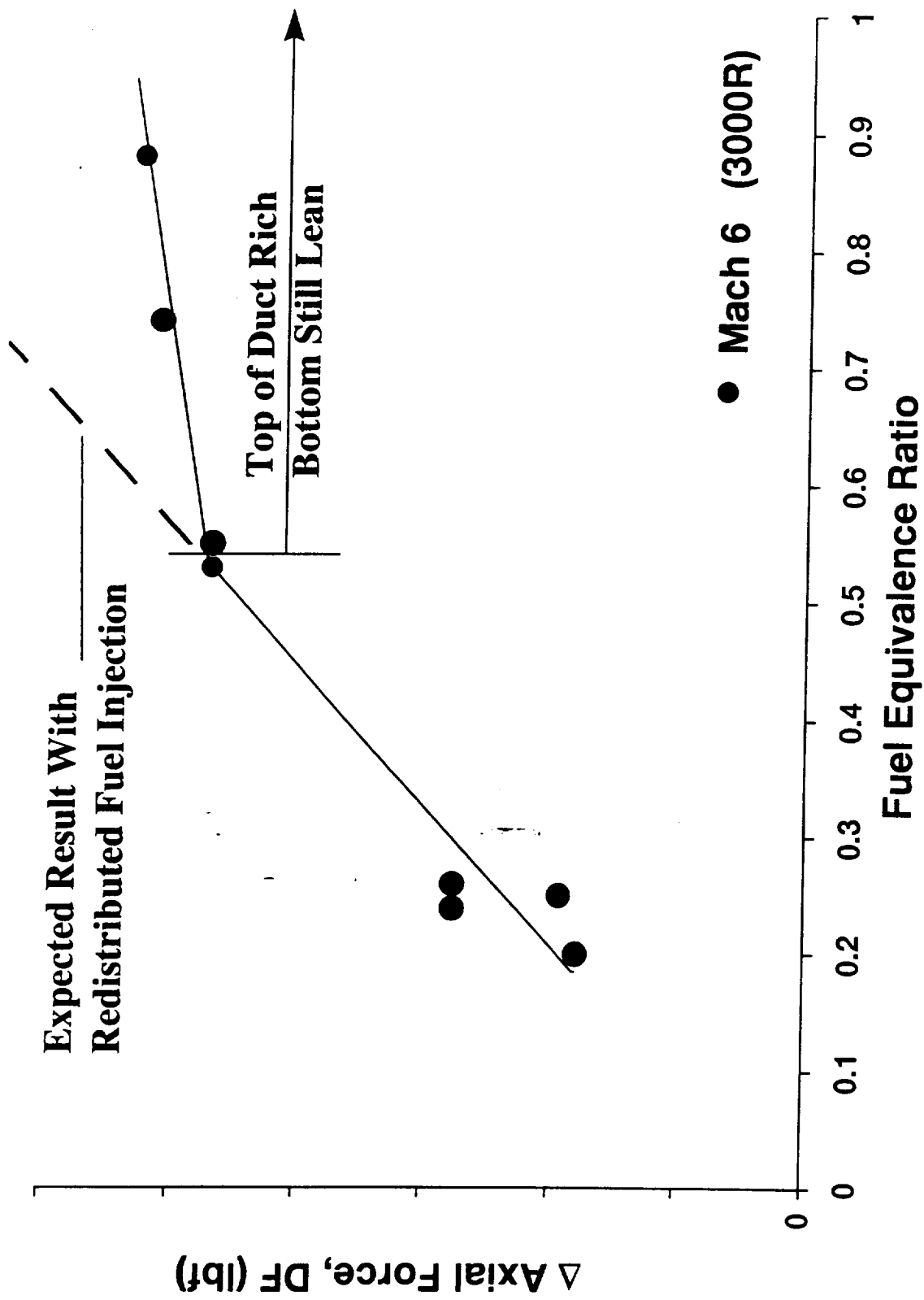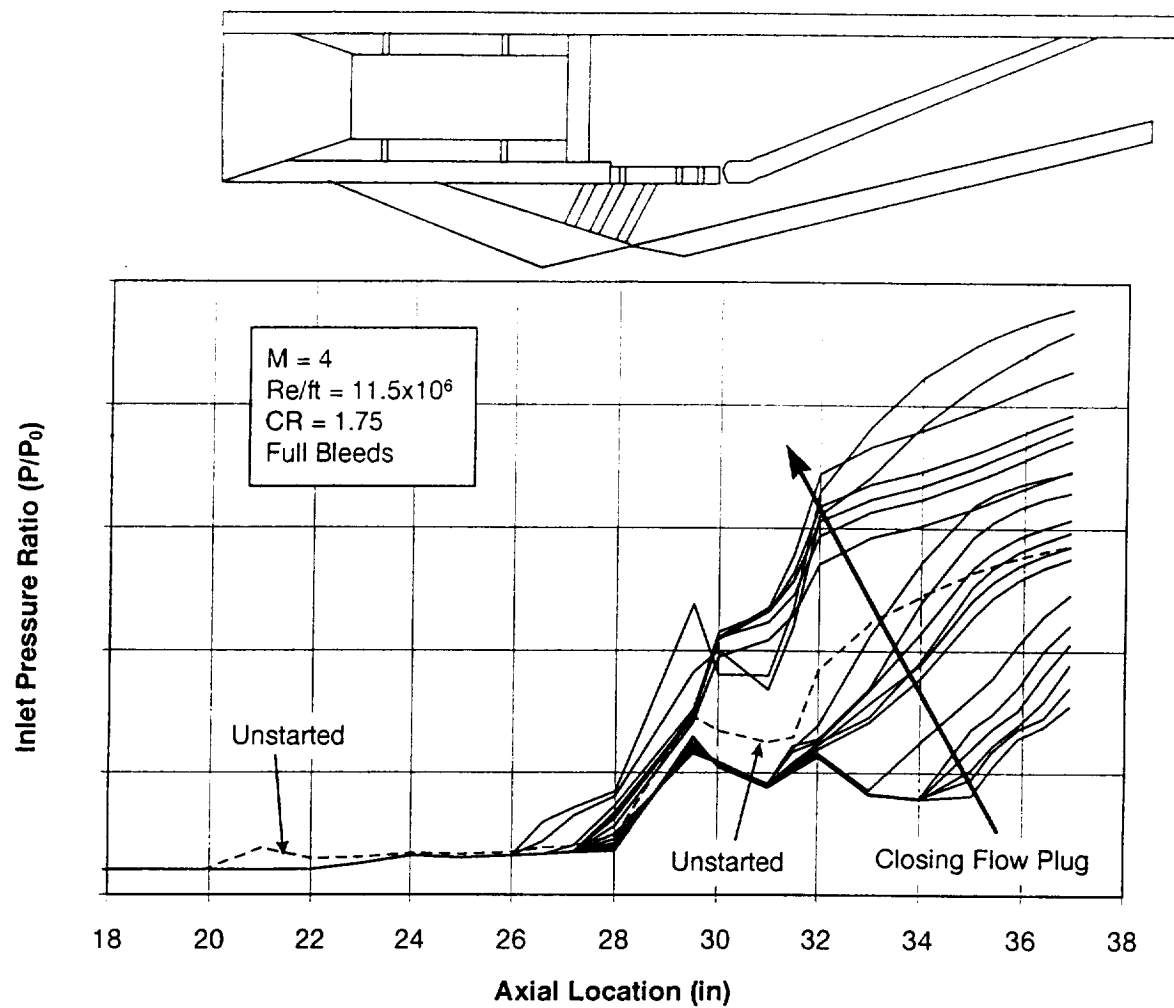
Figure 50

Figure 51

Figure 52
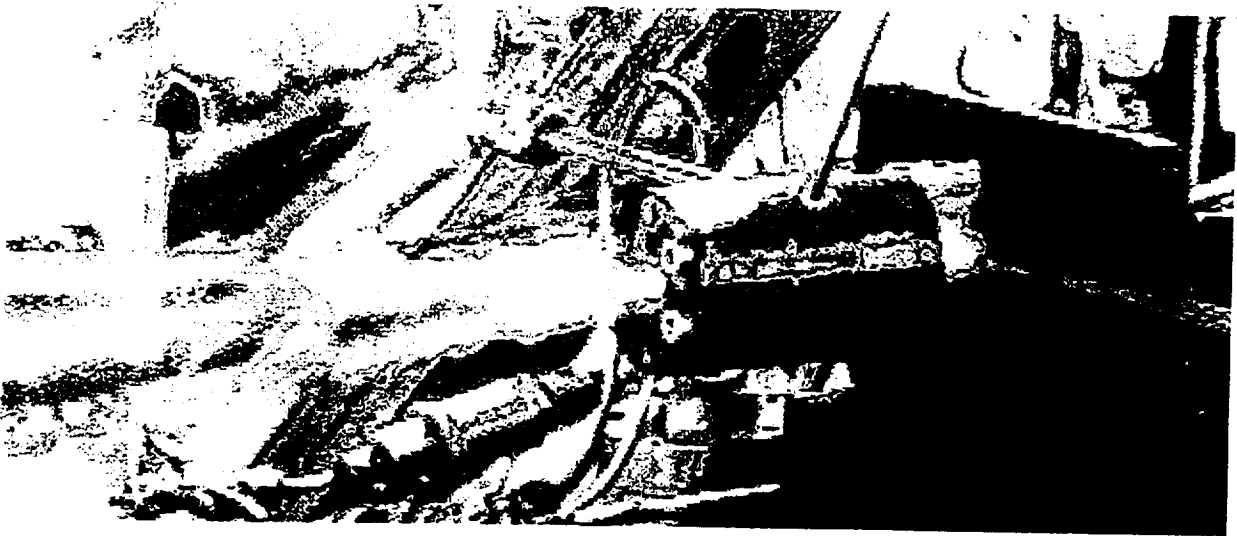
Figure 53
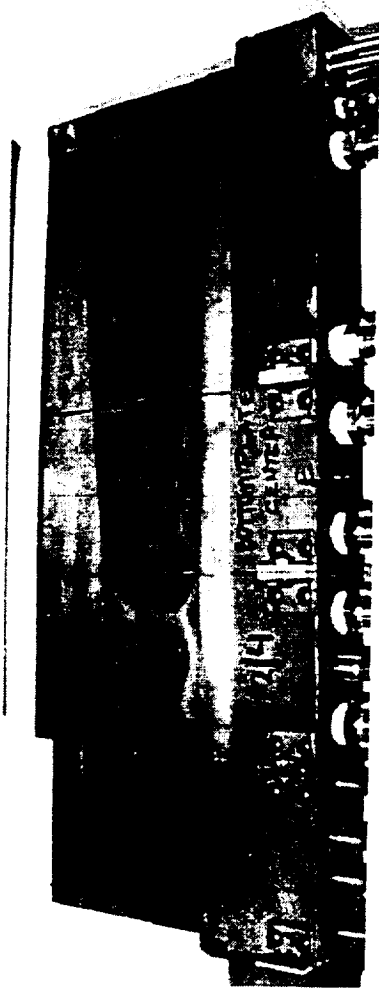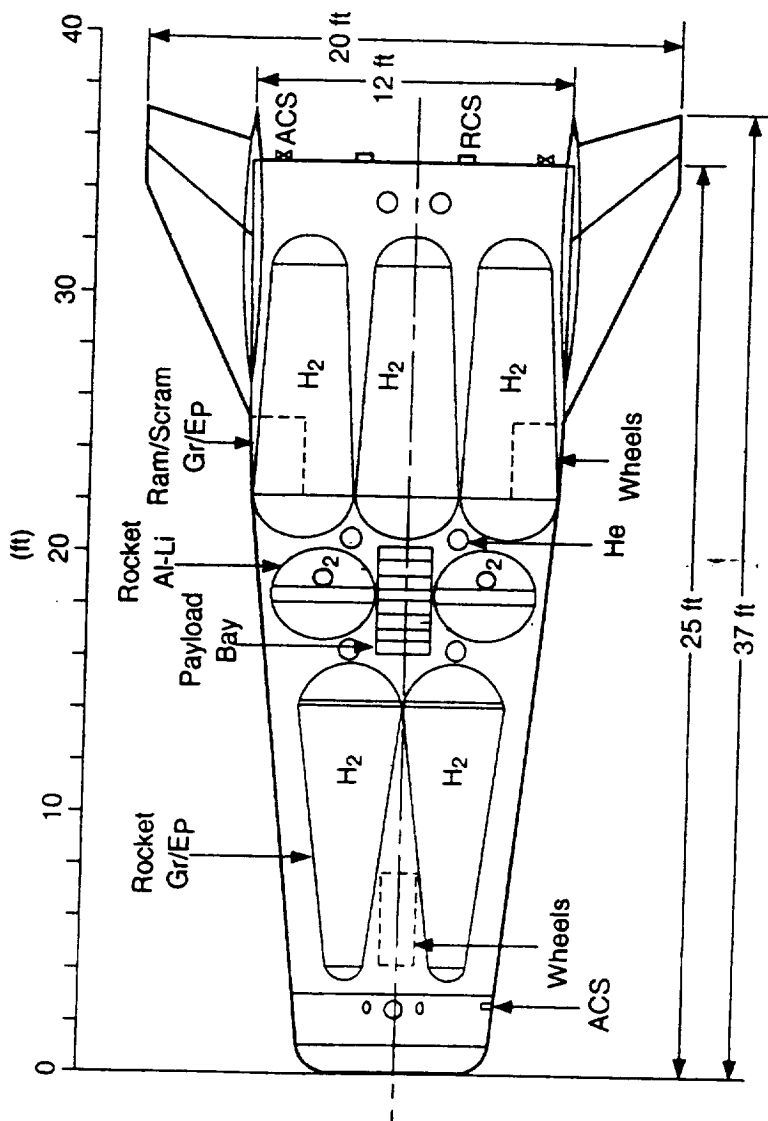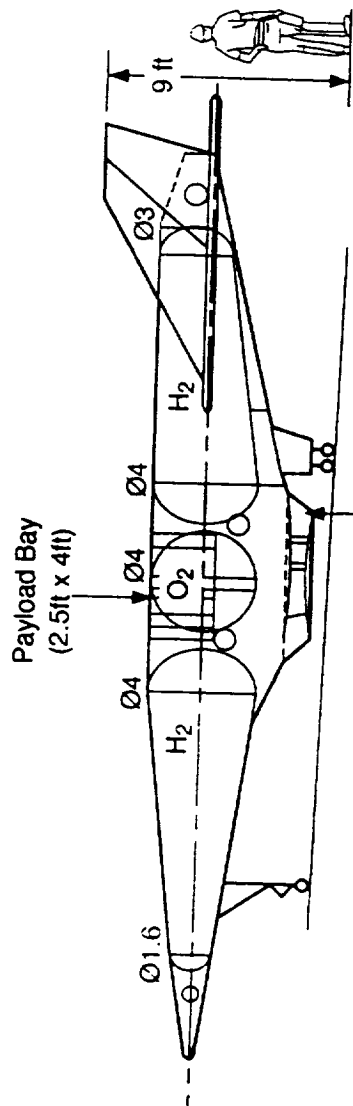
Figure 55

- m_O = 24,000 lbm
- Air Launched: M_{BO} = 10
- Ground Launched: M_{BO} = 7
- Sized for Maximum Burn Out Mach Number, M_{BO}

ACS
RCS
Payload Bay
F_{SL} = 19.6K lbf

40
(ft)
30
20
10
0

20 ft
12 ft
ACS
RCS

Rocket Al-Li
Ram/Scram Gr/EP

H_2
H_2
H_2

O_2
O_2
He Wheels

Payload Bay

Rocket Gr/EP

H_2
H_2

Wheels
ACS

25 ft
37 ft

9 ft

Ø3
H_2

Payload Bay (2.5ft x 4ft)

Ø4
O_2
Ø4

Ø4
H_2

RBCC
(F_{SL} = 2 x 9.8K = 19.6K lbf)

Ø1.6